Microscopy Investigations of Ash and Particulate Matter Accumulation in Diesel Particulate Filter Surface Pores

by

Daniel P. Beauboeuf

Submitted to the Department of Mechanical Engineering in Partial Fulfillment of the Requirements For the Degree of

Bachelor of Science in Mechanical Engineering
At the
Massachusetts Institute of Technology

May 2010
[June 2010]

Signature of Author:_____
Department of Mechanical Engineering
May 21, 2010

Certified by:_____
Alexander Sappok
Thesis Supervisor
Postdoctoral Associate

Certified by:_____
Victor Wong
Thesis Supervisor
Principal Research Scientist and Lecturer in Mechanical Engineering

Accepted by:_____
John H. Lienhard V
Collins Professor of Mechanical Engineering
Chairman, Undergraduate Thesis Committee

Microscopy Investigations of Ash and Particulate Matter Accumulation in Diesel Particulate Filter Surface Pores

by

Daniel P. Beauboeuf

Submitted to the Department of Mechanical Engineering in May 21, 2010 in Partial Fulfillment of the Requirements for the Degree of

BACHELOR OF SCIENCE IN MECHANICAL ENGINEERING

ABSTRACT

There has been increased focus on the environmental impact of automobile emissions in recent years. These environmental concerns have resulted in the creation of more stringent particulate matter emissions regulations in the United States and European Union. These limits have forced diesel engine manufacturers to reduce particulate matter (PM) emissions by an order of magnitude beginning in 2007. Diesel particulate filters (DPF) provide the most effective means of reducing PM emissions from diesel exhaust. DPFs can reduce over 99% of PM in the exhaust.

DPF effectiveness is limited by the accumulation of ash. Ash is comprised of incombustible material from engine lubricants. Engine oil additives based on P, Zn, S, Ca, and Mg are responsible for the majority of ash. Ash accumulation in DPFs reduces their useful life by plugging the filter's inlet channels. Ash deposition leads to increased pressure drop across the DPF, which reduces the engine's performance and negatively impacts fuel economy.

The process of ash accumulation in DPF channels is not well understood. This research is focused on exploring the ash interactions with DPF walls, pores, and the catalyst washcoat. Based on scanning electron microscopy analysis of ash loaded DPFs from the field and from filters loaded with ash in the laboratory, a mechanism for ash accumulation is presented.

Thesis Supervisor: Alexander Sappok
Title: Postdoctoral Associate

Thesis Supervisor: Victor Wong
Title: Principal Research Scientist and Lecturer in Mechanical Engineering

(This page intentionally left blank)

ACKNOWLEDGEMENTS

I would like to take this opportunity to thank the people that made my years at MIT memorable. MIT has been a wonderfully intense, difficult, and ultimately rewarding adventure.

I am very thankful to Dr. Alexander Sappok for bringing me on board in 2007 with what was his Ph.D. thesis work at that time. I was fortunate enough to be included in some of the work that became published. I would also like to thank Dr. Victor Wong for encouraging me to continue with this project throughout my undergraduate career. Staying in Sloan Automotive Laboratory was one of the best decisions I have made in my time at MIT. I am very fortunate for having the opportunity to work with Dr. Wong and Dr. Sappok.

I would also like to thank the MIT Consortium to Optimize Lubricant and Diesel Engines for Robust Emission Aftertreatment Systems, for creating this research opportunity, and opening doors for me.

I owe a debt of gratitude to my friends for their unwavering support during some of my must difficult times at MIT, and for creating many of the best times.

My family has been a blessing in my time here at MIT. Their sacrifices have given me the opportunity to realize dreams they could not. Their perseverance in the face of adversity is inspirational. My graduation from MIT is as much the result of their hard work and determination, as it is mine.

Lastly, I am blessed to have the opportunity to share this MIT experience with my girlfriend Maryelise. My time with her at MIT has been some of my happiest.

(This page intentionally left blank)

TABLE OF CONTENTS

LIST OF TABLES

LIST OF FIGURES

NOMENCLATURE

ATS	Aftertreatment System
Ca	Calcium
CI	Compression Ignition
CO	Carbon Monoxide
CO_2	Carbon Dioxide
DPF	Diesel Particulate Filter
EDX	Energy Dispersive X-ray Spectrometry
EGR	Exhaust Gas Recirculation
HC	Hydrocarbons
LNT	Lean NOx Trap
Mg	Magnesium
NO	Nitrogen Oxide
NO_X	Oxides of Nitrogen
P	Phosphorous
PM	Particulate Matter
PPM	Parts per Million
Re	Reynolds Number
S	Sulfur
SEM	Scanning Electron Microscope
SI	Spark Ignition
SO_2	Sulfur Dioxide
SO_4	Sulfate
TDC	Top Dead Center
ZDDP	Zinc Dialkyl-Dithio-Phosphate
Zn	Zinc

D_w	Hydraulic diameter
f	Fanning friction factor
k	Permeability
L	DPF length
P	Pressure
w	Porous media thickness
$Z_{In/Out}$	Channel inlet/outlet friction coefficient

ΔP_{Ash}	Ash layer pressure drop
$\Delta P_{Channel}$	Channel pressure drop
ΔP_{In}	Pressure drop due to inlet gas contraction
ΔP_{Out}	Pressure drop due to outlet gas expansion
ΔP_{Total}	Total DPF pressure drop
ΔP_{Soot}	Soot layer pressure drop

ΔP_{Wall}	Substrate wall pressure drop
ε	Porosity
μ	Dynamic viscosity
ν	Kinematic viscosity

1 INTRODUCTION

Diesel fuel is important in personal and commercial transportation. Diesel vehicles represent more than 40% of all passenger cars in Western Europe (in France, Austria, and Germany diesels power close to 60% of passenger cars) [1]. Diesel powers nearly all heavy freight transport because of their fuel economy and reliability. However, diesel engines emit particulate matter (PM), a regulated emission. Regulations in Europe and the United States of America require dramatic reductions in these emissions for 2007. Diesel Particulate Filters (DPF) have emerged as the preferred technology to reduce PM emissions.

While diesel engines have proven to be very reliable, DPFs cannot match the engine's useful life. DPFs become plugged with incombustable ash originating primarily from engine oil additives. As engine oil is consumed, the ash is carried with PM in the exhaust flow and builds up in the DPF. Ash accumulation over time increases backpressure, which robs the engine of power and reduces fuel economy. DPF plugging currently requires periodic cleaning or filter replacement, which is undesirable.

1.1 The Diesel Engine

Rudolph Diesel invented the diesel engine in the 1890s (German Patent 86,633 of March 30, 1895; US Patent 608,845 of August 9, 1898). It was known for being a "highly efficient, slow burning, compression ignition, internal combustion engine". Diesel engines are similar to gasoline engines in that they use a conventional cylinder and piston arrangement [2]. They rely on air heated by compression to ignite (CI) the fuel. This is the main difference from conventional spark ignition engines (SI), which rely on a spark plug to initiate combustion [4].

In the compression stroke, air is compressed to 3-5.5x10^6 Pa to increase cylinder temperature to between 700°C and 900°C. The high-pressure environment necessitates a very sturdy engine block design. Older engines injected fuel into a pre-chamber. There,

the fuel would be heated with a glow plug prior to traveling into the combustion chamber. Newer direct injection (DI) systems do away with the prechamber, reducing pumping losses and increasing fuel economy by as much as 10% to 15% [2]. Fuel that would have been left on the prechamber walls is used for combustion instead of being wasted. DI relies on timing injections near the top dead center (TDC) piston position to ensure that the fuel meets the air at the precise time when the air temperature and pressure are most conducive to efficient combustion.

1.1.1 Diesel Engine Advantages

Diesel engines compress air to high- pressure before injecting fuel. The high temperature environment of compressed air vaporizes the fuel, allowing it to mix. Diesel fuel combusts once it reaches the required temperature and pressure [3]. Diesel engines have compression ratios that can vary from 12 to 24, significantly higher than that of their SI counterparts. The diesel engines' high compression ratio combined with low pumping losses, a more energy dense fuel, lean combustion, and lower frictional result in a 20-40% fuel economy advantage compared to equivalent gasoline alternatives [4].

The lower frictional losses are the result of slow engine speeds. Diesel engines need to run slower to give the fuel- air mixture enough time to combust. The robust engine components and slow engine speeds mean that useful life of a diesel engine is three to four times that of comparable SI engines. Additionally, diesels produce lower carbon monoxide and hydrocarbon emissions than uncatalyzed SI engines [2]. Although engine components are designed for extended life cycles, current DPF aftertreatment systems cannot match engine longevity.

1.1.2 Diesel Emissions

Diesel engines generally have lower CO emissions than catalyzed gasoline engines. However, they emit higher levels of NOx and PM emissions than comparable SI engines with three way catalysts [2]. One of the major problems with diesels is that not only are

NOx and PM emissions higher, but there is a tradeoff between reducing one or the other. The lean combustion process makes NOx reduction difficult to address in- cylinder, since the cylinder environment is oxygen- rich. In- cylinder emission controls cannot meet current emissions regulations for both PM and NOx. It is necessary to use aftertreatment systems. Aftertreatment systems are PM and NOx reduction devices installed after the combustion chamber, usually in the exhaust piping.

PM is familiar to most people as the black smoke that comes out of the exhaust of early diesel vehicles. This PM consists of carbon, soluble organic fraction (SOF), sulfates, and ash. Current engine technology has allowed for greater control of the fuel air mixture in modern engines, which reduces this problem [2]. DPFs can further reduce PM by over 99% in some cases [4].

1.2 Diesel Emissions Regulations

In the past few decades, regulatory agencies have become more interested in reducing the human and environmental problems associated with vehicle pollution. Knowledge about how automobile emissions contribute to smog, ozone depletion, and global warming has improved. As a result, regulations were developed in an attempt to reduce harmful exhaust pollution. The United States Environmental Protection Agency (EPA) classifies the emissions of PM and ozone precursors from diesel engines as associated with serious health problems including premature mortality, aggravation of respiratory and cardiovascular disease, aggravation of existing asthma, acute respiratory symptoms, chronic bronchitis, decreased lung function, and a likely human carcinogen [6]. Additionally, PM in the form of black soot (produced from cooking, solid fuel, and diesel exhaust), is a major contributor to global warming. It could have up to 60% of the warming effect of carbon dioxide, making it the second most potent greenhouse gas. Black soot is a "dominant absorber of visible solar radiation in the atmosphere. Unlike carbon dioxide, which can stay in the atmosphere for more than a century, black soot only stays in the atmosphere for weeks." Therefore, efforts to reduce this PM emission have nearly instantaneous positive environmental impact [7].

Although the national PM levels have been decreasing since 1999 (when data collection began for PM pollution), there are over 250 areas of the United States with PM air quality in excess of healthy limits. Over 100 million people reside in these regions [4,6]. Diesel engines are responsible for most small particulate emissions, $PM_{2.5}$ (defined as PM smaller than 2.5 μm) in developed nations, including the United States. As a result, emissions regulations mandated a decrease in heavy- duty diesel PM emissions from 0.1g/HP-hr to 0.01g/HP-hr. This kind of reduction would not be possible without the adoption of ultra- low sulfur diesel (ULSD) fuel. The EPA mandated use of ULSD (with sulfur content of less than 15ppm) in 2006. ULSD allows for the use of aftertreatment systems. Without ULSD, aftertreatment NOx and PM systems would suffer from sulfur poisoning, significantly decreasing their useful life. The new 2010 emissions regulations reduce NOx and PM emissions by over 98% from 1990 levels by 2010 [4].

1.3 Diesel Particulate Filter (DPF)

DPFs are currently the most effective aftertreatment device for reducing PM emissions. They decrease PM by 99%, making DPFs the preferred option for meeting current and future vehicle emissions regulations (Figure 1.1). The amount of PM emitted without a DPF is two orders of magnitude higher than with a DPF. The DPFs currently on the market are made of a ceramic material, usually cordierite ($(Mg,Fe)_2Al_4Si_5O_{18}$) in heavy duty applications. DPFs may also contain a catalyst (Pt, Pd, Rh, or V) to help reduce the activation energy required to regenerate PM. The DPFs are generally wall- flow filters, with a honeycomb structure and porous walls. The channels are blocked at either the inlet or outlet, to force exhaust gases to travel through the pores. The escaping gas leaves PM behind in the filter, and along the inlet channel walls (Figure 1.2).

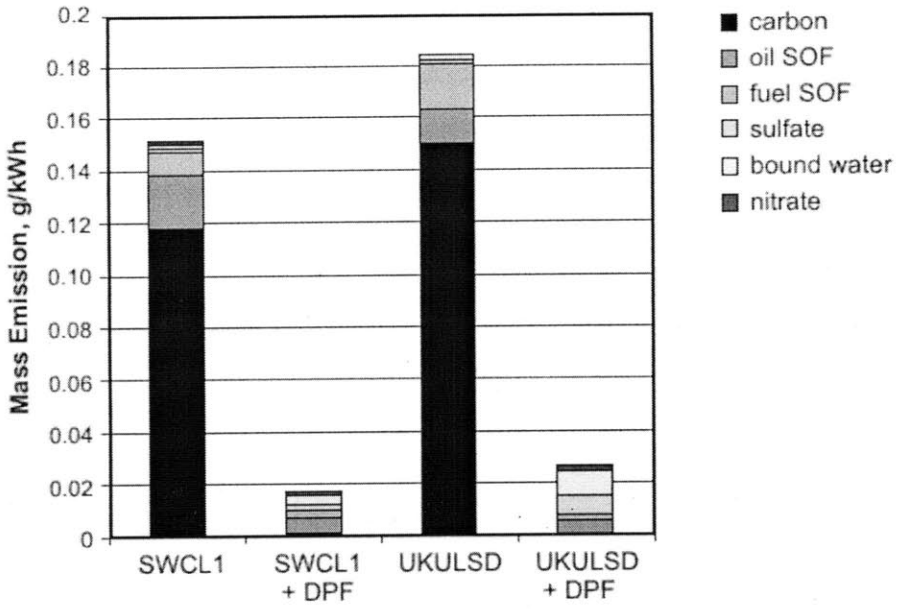

Figure 1.1. PM and SOF emissions are reduced with DPF use. [8]

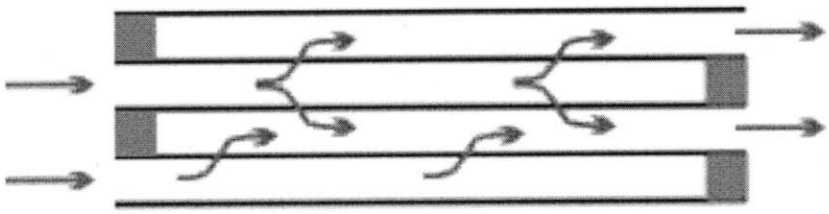

Figure 1.2. Exhaust flow through DPF channels. [8]

PM accumulates in the DPF over time, restricting flow and increasing backpressure. The majority of this soot can be burnt off through a process called regeneration. Regeneration oxidizes PM into CO, CO_2, and ash.

There are two methods of regeneration, active and passive. Active regeneration is the process by which the DPF is heated until the inlet temperature is above the soot oxidation temperature (~600°C). Passive regeneration also involves adding catalytic materials to reduce the activation energy for oxidation. However instead of relying on periodic inlet temperature increases, regeneration is initiated at a much lower temperature and can occur continuously. Most manufacturers use a combination of active and passive regeneration.

Some incombustible material, ash, remains after DPF regeneration. This material creates an ash layer that eventually plugs the DPF channels. The accumulation of ash eventually increases backpressure, taxing engine performance. Ash accumulation limits DPFs service life. Ash deposits in DPF channels currently require removal for cleaning or replacement (Figure 1.3).

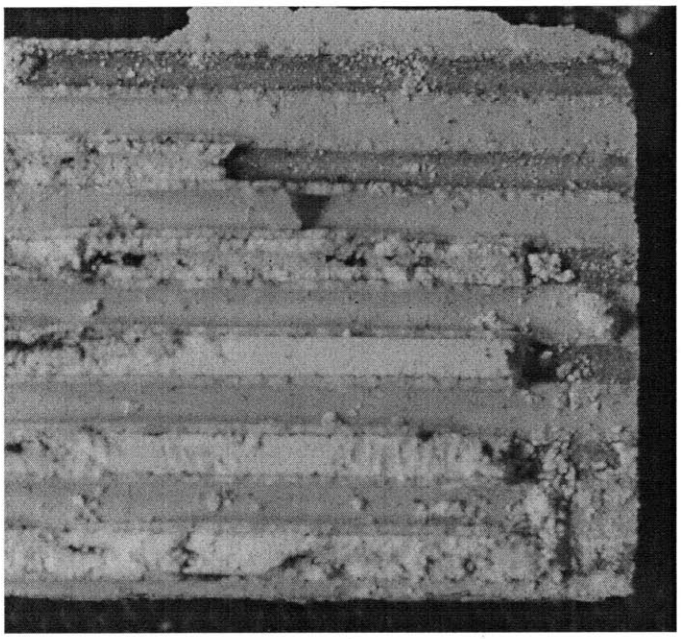

Figure 1.3. Ash plugs DPF inlet channels.

Figure 1.3 illustrates the problem of ash accumulation. The ash lines the inlet channel walls of the DPF. Some of the ash forms a plug in the back of the DPF. Over time the plug grows, and reduces the DPF's effective length. This means the engine has to work harder to push its exhaust through the filter. The ash problem is the source of pressure drop associated with DPFs [4].

1.3.1 Pressure Drop Fundamentals

The pressure drop across the DPF can be modeled in parts, as:

$$\Delta P_{DPF} = \Delta P_{in} + \Delta P_{out} + \Delta P_{channel} + \Delta P_{wall} + \Delta P_{ash} + \Delta P_{PM}, \quad (1.1)$$

where the ΔP_{in} and ΔP_{out} are due to the change in pressure from expansion and contraction of the eshaust gases at the DPF inlet and outlet. $\Delta P_{channel}$ is the pressure drop due to surface drag losses of the flow in the channels. This can be estimated via the pipe flow pressure drop equation for a conduit:

$$\Delta P_{channel} = 4f\left(\frac{L}{D_W}\right)\left(\frac{\rho v^2}{2}\right) \tag{1.2}$$

where D_w is the wetted diameter, ρ is the viscosity, and f is the friction factor. The friction factor is found by

$$f = \frac{K}{\mathrm{Re}} \tag{1.3}$$

where K=14.23 for conduits with a square cross section and Re is the Reynolds number.

Darcy's law governs the pressure drop for flows through porous media, such as the DPF walls, ash, and PM. Ash and soot accumulation in the DPF increases the thickness of the porous layer, which is reflected in the overall layer permeability term K_p,

$$\Delta P_{Wall/Ash/Soot} = \left(\frac{\mu}{K_P}\right)\cdot v_w \cdot w \tag{1.4}$$

where μ is the gas dynamic viscosity, and w is the ash/ PM layer thickness. K_p is the permeability is related to pore geometry (length, width, and depth). K_p is an intensive property of the porous medium that is directly proportional to porosity and pore diameter of the material. It is dependent upon not only the pore size in the DPF wall, but changes when ash or soot accumulates in pores. Ash porosity and mean pore size are both functions that create K_p. The mechanisms controlling both ash packing and ash particle size are not well understood. Ash layer permeability has been calculated based on the

relations of the permeability of porous media as a function of porosity. The most common relation for DPF ash and soot permeability modeling is the Rumpf and Gupte relation. It is limited in that the "relationship was based on experiments utilizing uniformly random packs of spherical particles of a porosity range from 0.35 to 0.7, with Reynolds numbers from 10^{-2} to 10^{2} [4]."

$$K_p = 5.6^{-1}\varepsilon^{5.5}d_p^{2}, \tag{1.5}$$

where ε is the overall porosity

$$\varepsilon = 1 - \frac{\rho_{Packing}}{\rho_{Theoretical}}, \tag{1.6}$$

and d_p is the average sphere diameter (Rumpf and Gupte used particles with diameters ranging from $d_{p,\,min}/d_{p,\,max} = 1/7$). The permeability of a porous material is directly related to the porosity and pore diameter of the material. For DPFs, K_p is a major contributor to the pressure drop from the wall, ash and PM, which itself is the largest contributor to overall DPF pressure drop. The amount and location of ash in surface pores and on the inlet channel wall has a large effect on pore geometry, and thereby on K_p [3]. Further, ash effectively reduces overall porosity, which also reduces K_p. Since K_p is inversely proportional to wall, ash, and PM pressure drop, decreasing K_p increases pressure drop.

1.3.2 Ash Accumulation

Ash is generated from the consumption of engine lubricant, engine wear and corrosion, and trace metals in the fuel. The majority of ash comes from the 12-18% of oil consisting of inorganic additives. Additives play an important role in reducing engine wear, reducing corrosion, and other functions in the engine. Common additives consist of calcium, magnesium, and zincdialkyl-dithio-phosphates (ZDDP) [9]. The resultant ash is generally Ca, Zn, P, Mg, and S compounds, usually forming phosphates, sulfates, and oxides [4]. Current regulations limit the amount of additive content in engine oil (CJ-4 oil). Sulfated ash content must be less than 1%, phosphorus less than 0.12%, sulfur

content less than 0.4%, maximum volatility less than 13% [10]. Even with CJ-4 oil, ash accumulation is still a major problem for aftertreatment devices.

Figure 1.4 illustrates the importance of understanding the initial stages of ash accumulation in DPF life. The first few ash deposits after early regeneration cycles are responsible for more of the pressure drop than all the ash that accumulates afterward. Figure 1.4 measures pressure drop versus ash load for two cordierite DPFs with platinum catalysts loaded with CJ-4 ash. The majority of pressure drop over the entire life of the DPF is due to the ash accumulated in pores (depth filtration). At 33g/L of ash load, depth filtration accounts for 6% of total ash, and 40-60% of total pressure drop [4].

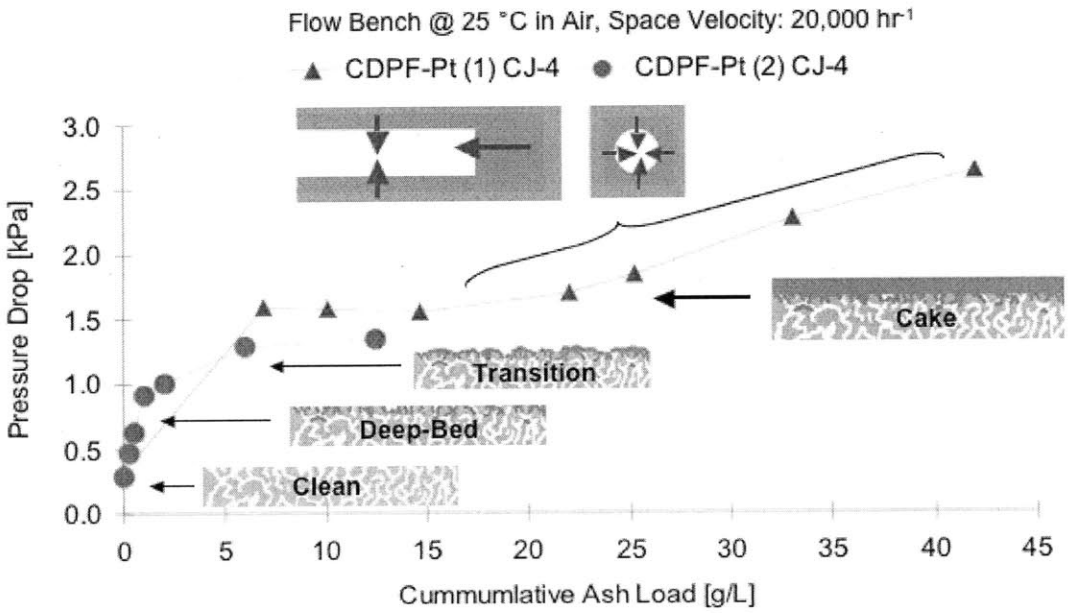

Figure 1.4. Pressure drop as function of ash load. [4]

1.4 Motivation

The mechanisms for ash collection in the DPF are not well understood. Pressure drop data suggests that the location of ash and soot in wall pores, accumulated in the beginning of DPF life is, responsible for creating much of the pressure drop increase observed in Figure 1.4 over the course of DPF life. The first regenerations are unique in that at this stage, some amount of soot collects in the DPF wall pores. The pore accumulation has the largest effect on pressure drop because it reduces overall porosity, increasing pressure

drop from wall pores, ash, and PM- a major contributor to overall pressure drop. It is necessary to understand the manner in which ash and soot collects in the DPF surface pores to better understand the DPF's pressure drop performance.

1.4.1 Current Understanding of PM Accumulation

Since ash comprises 1% of total PM emissions, and ash is transported by PM, it is necessary to first understand PM accumulation before understanding the resulting ash properties. When a DPF is new, PM comes into contact with the DPF channel surface (Figure 1.4). At elevated ash loads above 10 g/L, ash may coat the filter walls forming a barrier between the substrate and soot cake. The ceramic DPF material has porous channel walls. The pores fill with PM first, then a soot cake layer. This layer coats the entire channel surface. It can be hundreds of μm thick [11].

The amount of PM that travels into pores deep in the wall material is minimal. Most accumulation that is considered "depth" filtration is actually due to the filling of surface pores. As a result, very few nano- scale particles actually filter deep into the DPF wall. PM generally stays within a few pore diameters of the filter surface (Figures 1.5-1.9) [11].

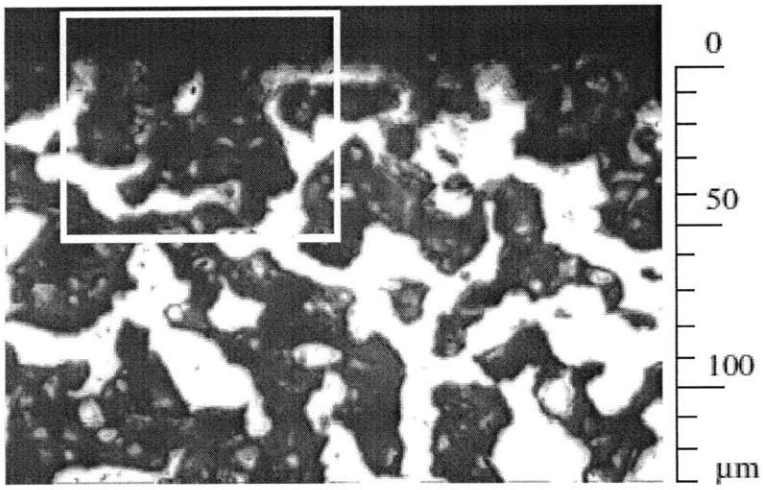

(a) Time = 0

Figure 1.5. Cross-section of an inlet channel. The boxed area is a pore exposed to the inlet flow. This photograph was taken before exhaust gas flow began. [11]

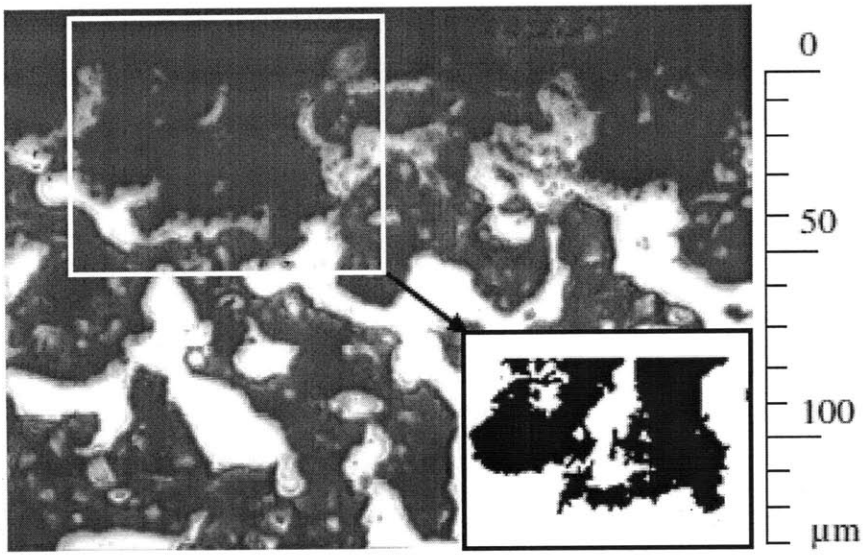

(b) Time = 1 minute

Figure 1.6. After 1 minute of exhaust flow, the surface pore is full of PM. [11]

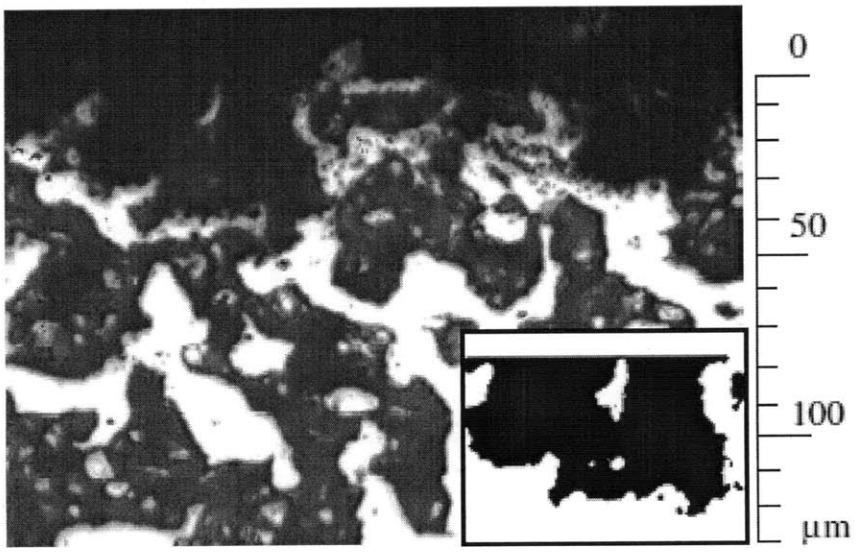

(c) Time = 5 minutes

Figure 1.7 After 5 minutes of exhaust flow, the soot cake layer has formed on the DPF channel surface. The filled surface pores restrict depth filtration. [11]

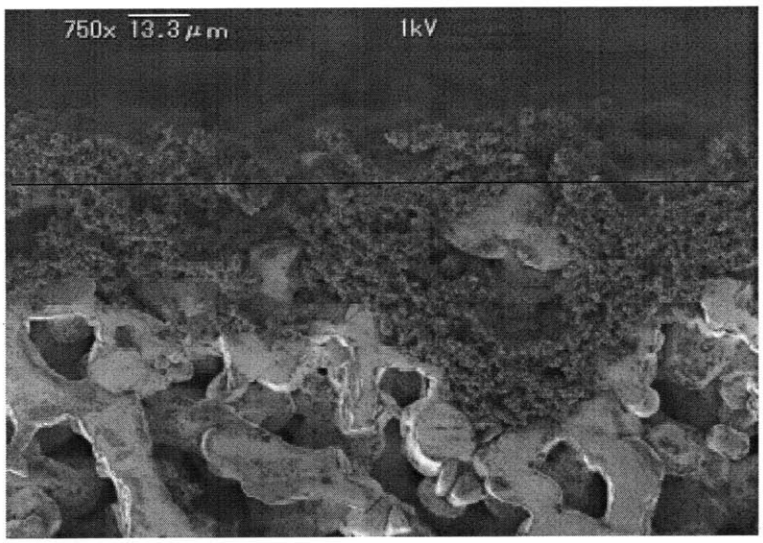

Figure 1.8. Sampled viewed via SEM. The surface pores are full, while immediately adjacent pores are empty. The soot cake has formed. [11]

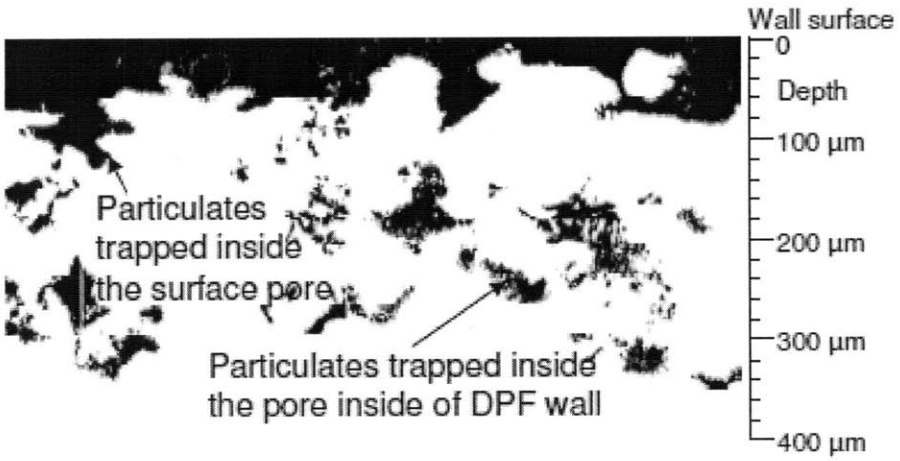

Figure 1.9. Some small amount of PM is trapped inside the wall. [11]

Figures 1.5-1.9 illustrate the process of PM accumulation in DPF channels. The first stage is what is commonly referred to as depth filtration. This is the initial stage of PM accumulation in which surface pores collect most of the PM. After a short time (5 minutes) the surface pores are full, and PM is forced to create a soot cake layer on the DPF channel surface. The soot cake prevents more depth filtration. Most PM trapped by a DPF is collected in the soot cake. Therefore, it is likely that most of the ash that accumulates is also in the soot cake layer, and not in DPF pores.

1.5 Objectives

Based on the data presented in the literature and previous work at MIT, the following theory is proposed to describe the initial stages of ash accumulation in the DPF. Ash is transported to the DPF and deposited with PM. Ash comprises less than 1% of the total PM emissions in exhaust. Because of the relatively low amount of ash in PM, and the fact that most PM accumulates on the channel wall, ash retention in surface pores should be minimal. Ash accumulation should occur mostly on the DPF surface. Negligible amounts of ash should accumulate in pores.

In order to test this theory, DPF samples must be tested for the presence of ash in surface pores. Scanning electron microscopy (SEM) imaging and elemental analysis using energy dispersive X-Ray spectrometry (EDX) provide useful tools to determine whether ash is present in surface pores and adjacent wall pores. If ash is detected deep inside the DPF wall, it suggests that ash deposits differently than soot, and negates the theory.

Additionally, determining the ash porosity provides quantitative information to support the image analysis and improve predictions of ash contribution to pressure drop. Mercury porosimetry and SEM image porosity analysis present potential measurement techniques to obtain this quantitative information

2 TEST SET-UP AND EXPERIMENTAL PROCEDURES

Samples from field- aged and lab- aged DPFs were used in this study. Analysis included SEM imaging, and EDX elemental analysis. SEM imaging shows where ash accumulates on the DPF wall with high resolution. EDX scans the SEM images to determine the relative concentration of elements of interest in surface pores and along the channel walls. For this analysis, P, Mg, Zn, Al, S, Si, O, and Ca were the focus of the EDX analysis. The results in subsequent sections discuss the measured P, Ca, Zn, and S distribution. Since cordierite is made of Si and Mg, the EDX maps of those elements served as a reference to identify where the DPF material ends and the ash layer begins. Aluminum was detected because the field washcoats also contained an Al binder.

Another useful EDX feature included in the results is the line scan. It allows for comparison of elemental composition along a specified path. For example, when comparing the amount of ash in a DPF pore, versus the amount of ash on the channel surface, line scans are helpful in identifying which elements appear in different areas of a sample. The line scan feature of the EDX analysis was used to investigate distribution of elements in the DPF walls. The resulting data relates the amount of various elements with position along the path. Line scans also reveal void space in the ash layer. The fraction of void space to ash in the layer could be useful for porosity measurements.

Unfortunately, porosity measurements could not be taken because of persistent mercury porosimeter malfunctions at both the MIT Center for Materials Science and Engineering (CMSE) and the Institute for Soldier Nanotechnology (ISN) rendered both porosimeters non-functional for the duration of the spring semester 2010. This information would be extremely useful, and should be the focus of future work.

2.1 Key Test Parameters

Cordierite DPFs were used for all the lab tests. The lab- aged DPFs were loaded with ash via the accelerated ash loading system developed at MIT Sloan Automotive Laboratory[1]. The lab filters measured D5.66" x 6" (D14.38 x 15.24 cm). The lab- aged DPFs contained platinum- based catalysts. The field- aged DPFs were also cordierite. The field- aged DPFs were also catalyzed. The DPFs were loaded with CJ-4 oil. The filter cell geometry was 200 cells per square inch (31 cells/cm), 0.012-inch (0.3mm) wall thickness. Table 2.1 describes the amount of ash that accumulated by the time each sample was taken. Table 2.2 details the oil formulation for each sample. The base oil without additives is included in Table 2.2 to indicate the change in Ca, P, S, or Zn levels. No samples were loaded with base oil alone were analyzed in this study.

Table 2.1. Filter ash load data and lubricants used to generate the ash. All samples were regenerated periodically.

DPF	Ash Level [g/L]	Lubricant	Regeneration
MIT Lab- aged	42	CJ-4	Periodic
MIT Lab- aged	28	ZDDP	Periodic
MIT Lab- aged	29	Ca	Periodic
Field (Regenerated)	~180,000 miles	CJ-4	Periodic
Field (Unregenerated)	~180,000 miles	CJ-4	Periodic

[1] The accelerated ash loading and aftertreatment system was designed to load a D5.66" x 6" DPF to 40 g/L of ash in under 100 hours. This ash load corresponds to roughly 300,000 miles of on- road use [3].

Table 2.2. Lab- aged DPFs used CJ-4 oil, or specific formulations of base oil with an additive.

Lab DPFs	ASTM D5185							
Lubricant	B [ppm]	Ca [ppm]	Fe [ppm]	Mg [ppm]	P [ppm]	Zn [ppm]	S [ppm]	Mo [ppm]
CJ-4	586	1388	2	355	985	1226	3200	77
Base Oil	1	<1	<1	8	2	<1	60	<1
Base Oil + Ca	3	2928	1	5	2	<1	609	<1
Base Oil + ZDDP	1	<1	<1	<1	2530	2612	6901	<1

There were three lab- aged DPFs analyzed in this study. The first was loaded with 42g/L of CJ-4 ash. The CJ-4 has a formulation that features 1388ppm of Ca, 1226ppm of Zn, 3200ppm of S, and 355ppm of Mg. Its expected that all of these additives will be present in the ash.

The second lab- aged DPF was loaded to 28g/L of base oil containing only ZDDP additives formulated to the 1% sulfated ash level. The other major additives are present in trace amounts. It expected that the ash will comprise of mostly Zn and P in this sample.

The third lab- aged DPF had 29 g/L of ash . The lubricant was made of the base oil with Ca additives. This formulation had 2928 ppm of Ca, 609 ppm of S, and was also formulated to the 1% sulfated ash level. This sample is expected to have ash with high levels of Ca and S, and low levels of Zn and P. Both field samples were loaded with CJ-4 oil. It is expected that all major additives (Ca, Zn, P, and S) will be present in ash from these samples.

2.2 Test Setup

2.2.1 Sample Preparation

DPF samples were taken from the center of the filters since the ash accumulation is most regular in the center of the DPF (where the radius is near zero in the circular plane of the cylindrical DPF). Cores were taken from the middle or rear of the DPF's axial length because the ash layer is thicker, or completely plugs the channel closer to the end of the DPF. The cores were ~1" in length, though most samples were shortened to fit in the epoxy dish (Figure 2.1).

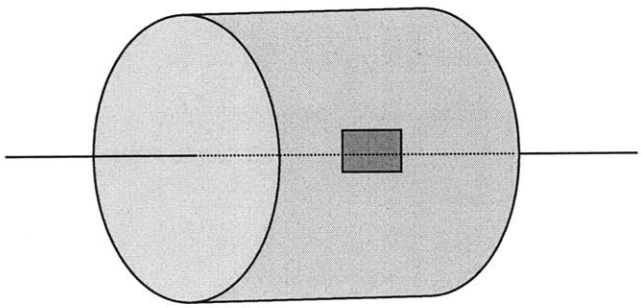

Figure 2.1. Rectangular DPF cores were taken from the center of the DPF's circular face.

The process of cutting a core must be done with care so as not to disturb the ash from its position in the channels (Figure 2.2). The ash is a powdery substance that can be disturbed by movement.

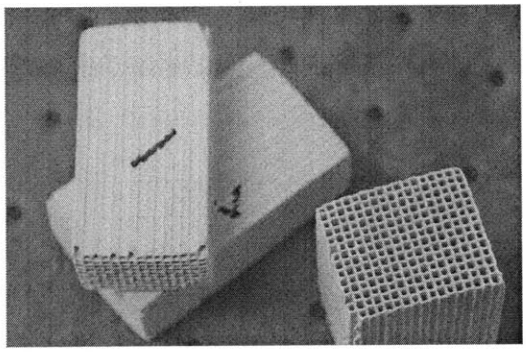

Figure 2.2. DPF cores without ash cut to the required dimensions for epoxy coating.

After the samples were removed, they were coated in epoxy to improve SEM image resolution. The epoxy also keeps the ash in place. The sample cores are placed in a 1.25" D x 0.5" depth dish. Epoxy must be poured into the dish one drop at a time so that it does not push the ash out of the channels. Once the epoxy hardens, the surface of interest is polished to a 5nm finish and then coated with a 50nm layer of carbon (Figure 2.3). Grinding the epoxy surface with 500, 1200, and 4000 grit sandpaper respectively, prior to carbon coating creates the required finish. It is important to note that the side of interest for SEM imaging must be facing down in the dish. The carbon coating is necessary to prevent the surface from charging under the electron beam of the SEM. Unfortunately, the carbon makes observing carbon accumulation impossible via EDX with these samples. It is possible to coat the epoxy samples with gold at the Center for Materials Science and Engineering (CMSE), which could be used to observe soot accumulation in future studies.

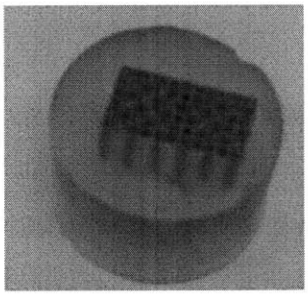

Figure 2.3. DPF core after epoxy coating. This sample has some channels that are plugged with ash. The epoxy allows for a fine surface finish for carbon coating, which improves SEM and EDX quality.

2.2.2 SEM Analysis

Image analysis was conducted with a JEOL 5910 general purpose SEM. It was used to map the ash accumulation on the channel walls and in pores. It provides high resolution (approximately 1nm), high magnification images. The magnification of the images presented here ranged from 100x to 1000x. The acceleration voltage was 15kV. These images were inspected using EDX to identify where specific elements in the ash

accumulate, and where those elements travel in the DPF wall. All electron microscopy analysis was conducted at the CMSE.

Individual channels were chosen from each sample for imaging and EDX. Afterward, smaller sections were chosen for high magnification EDX analysis. The high magnification images focused on the ash- washcoat- pore- wall interfaces. Line scans were used to quantify the relative elemental distribution in the wall, washcoat, and ash layer.

2.2.3 Porosimetry Measurements

Getting porosity measurements is essential for completing this dataset in the future. The ISN now has a functioning mercury porosimeter that is available to the MIT community for use. The Micrometrics Autopor IV 9500 measures the pore size and density of porous materials by surrounding them with Hg. The Hg fills the pores while the porosimeter measures the surface tension as a function of both time and distance around the sample. It is useful for pore sizes between 60nm and several hundred microns. There is some uncertainty with this method because the Hg flow may disturb the ash, distorting the data.

Porosity can also be measured using the SEM images of the samples because there is a difference in contrast between pores (void space) and gray material (ash and DPF wall). The results of this type of analysis have been statistically tested to the 95% confidence level for other nano-scale samples. Essentially, the imaging program sets a brightness threshold, above which is considered material, and below which is void space for calculating porosity[12]. There is some uncertainty in the results from this method due to errors in setting thresholds and errors in brightness/ contrast settings [13].

3 RESULTS

3.1 Lab- Aged CJ-4 DPF

This DPF was loaded with 42 g/L of ash using the accelerated ash loading system developed at MIT Sloan Automotive Laboratory. The CJ-4 is expected to create an ash layer composed of all major additives (Ca, Zn, P, Mg, and S).

3.1.1 SEM and EDX Images of Inlet Channel

The top left image in Figure 3.1 is the reference SEM image of one corner in the DPF inlet channel. The images labeled with the names of elements are the maps that the EDX analysis creates based on the concentration of each element it detects in the SEM image. Si is included as a reference to indicate where the DPF wall is located.

The EDX maps reveal that Zn deposits uniformly in the ash layer. The P was also uniform and its accumulation corresponds well with the Zn accumulation. This pattern suggests that a significant portion of the ash layer is composed of zinc phosphates. Trace amounts of S appear in the ash collected along the DPF wall (the S observed throughout the image is due to background levels, without an observably elevated concentration in ash layer). However, there are some bright spots of S that coincide with some of the bright Ca areas. Otherwise Ca appears fairly uniformly dispersed. This pattern implies some calcium sulfate in the ash. The Ca image indicates there are more high concentration Ca areas than high concentration S areas. Some of the high concentration Ca regions match those for P, suggesting that calcium phosphate may also be present.

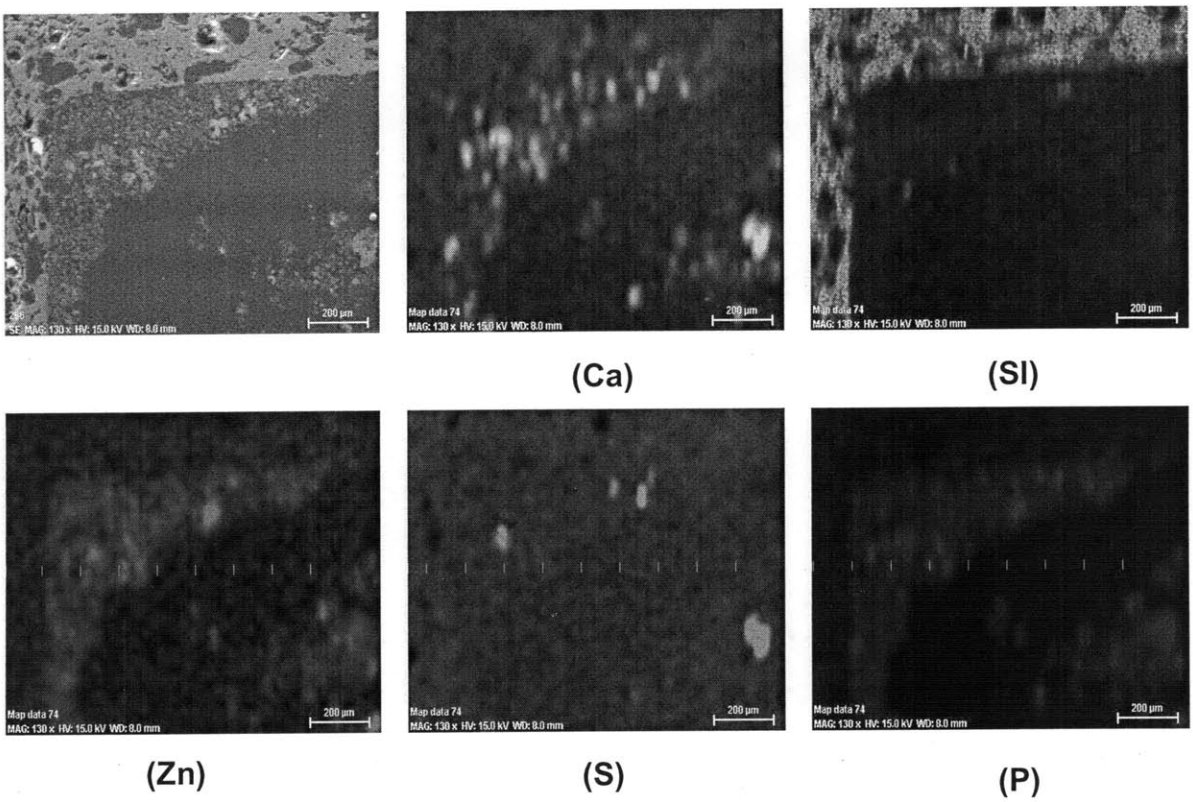

Figure 3.1. Lab- aged DPF with 42 g/L of ash from CJ-4 oil. SEM and EDX maps of one corner of DPF channel.

3.1.2 SEM and EDX Images of Surface Pore

A surface pore from the CJ-4 lab- aged DPF was chosen for further analysis. High magnification (500x) EDX analysis would show any ash collection in the pore. The SEM image shows a surface pore in contact with the ash layer (Figure 3.2).

At this magnification, it is apparent that Zn (and all of the ash for that matter) is accumulating strictly outside of the surface pore. As in the lower magnification image (Figure 3.1), the P accumulation areas appear to match those of the Zn. There is a distinct high concentration region in the lower center of the Zn image that is perfectly matched to the P image. This confirms the observations in the previous example, that a zinc phosphate compound is present in the ash. Additionally, the Ca has a non- uniform accumulation. There are high concentration regions in the ash layer, and none in the surface pore. The some of the Ca high concentration areas coincide with S, suggesting calcium sulfate in the ash, while others correspond with P.

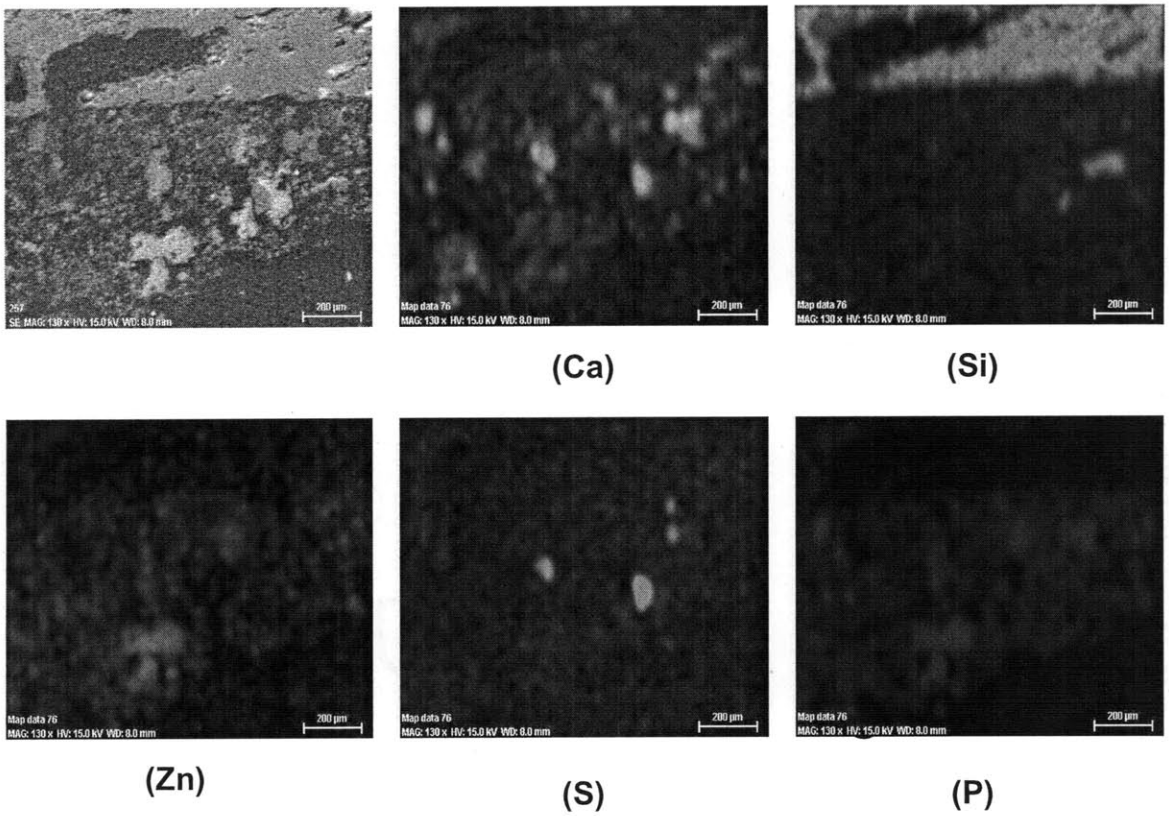

Figure 3.2. Lab- aged DPF with 42 g/L of ash from CJ-4 oil. SEM and EDX images of surface pore- ash layer interface.

3.1.3 Line Scan of Surface Pore

The line scan measures the relative concentration of each element along a specific path. The path for this sample was chosen to measure ash deposition in the DPF wall pores, surface pores, and in the ash layer. The line in Figure 3.3 begins in what is known to be cordierite in the DPF wall. The path goes through a large pore with an opening that is in contact with the ash layer. The path leads through the layer and into the open inlet flow channel.

Figure 3.3. Lab- aged DPF with 42 g/L of ash from CJ-4 oil. Line scan path.

The surface pore is located between the 100- 200 μm position on the line scan graph (Figure 3.4). The low levels of S, Mg, P, and Zn between 100-200 μm indicate that no significant amount of ash is collected in this pore. The ash layer is ~200μm thick immediately adjacent to the pore (Figure 3.4). There are some voids in the ash layer, specifically at 250μm and 320μm, which indicates that the ash also has some porosity. These voids could be used to determine overall ash porosity via SEM image analysis.

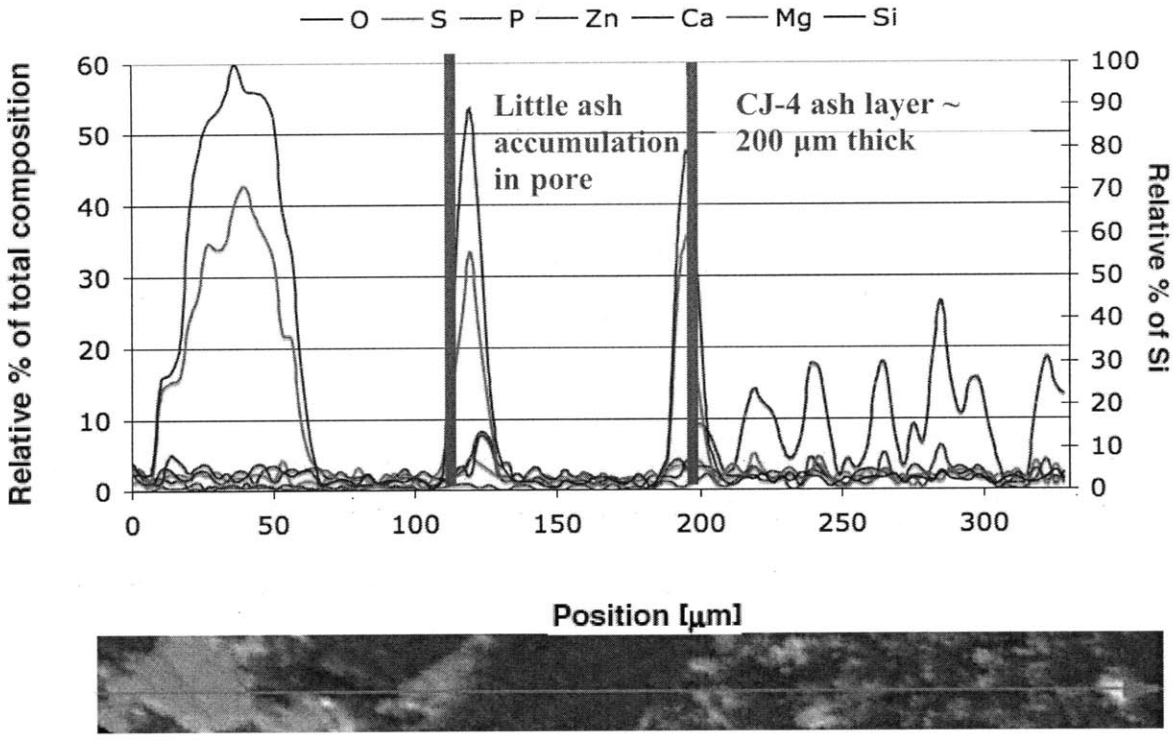

Figure 3.4. Lab- aged DPF with 42 g/L of ash from CJ-4 oil. The line scans show the relative concentration of each element by position along the scan path.

3.1.4 Summary of Observations for Lab- Aged DPF with CJ-4 Oil

Based on the analysis of the ash accumulation in the DPF channel, along the wall, and near surface pores, the following summarizes the general observations:

- Zn and Ca accumulate uniformly in the ash layer
- Ca is present in small areas, and appears to correspond with areas of S accumulation. This suggests that calcium sulfate is present in the ash
- P accumulation is uniform and corresponds well with Zn, suggesting some of the ash is zinc phosphate
- Some high concentration P areas coincide with Ca, so calcium sulfate may also be in the ash
- Ash primarily covered the surface pores, no significant ash accumulation in the pores

3.2 Lab- Aged DPF with Ca Additive

The following analysis was conducted on a DPF sample loaded with the base oil containing only a Ca additive. This oil formulation contained primarily Ca and S and was formulated to the 1% sulfated ash level.

3.2.1 SEM and EDX Images of Inlet Channel

Zn EDX images are not included because this oil did not contain any appreciable levels of Zn. Si and Mg define the cordierite wall in the images. The P image is unclear, with the exception of a few high concentration areas against the channel wall. This suggests that there are trace amounts of P in the sample, but the P that is present accumulates only in specific regions in the ash layer (Figure 3.5).

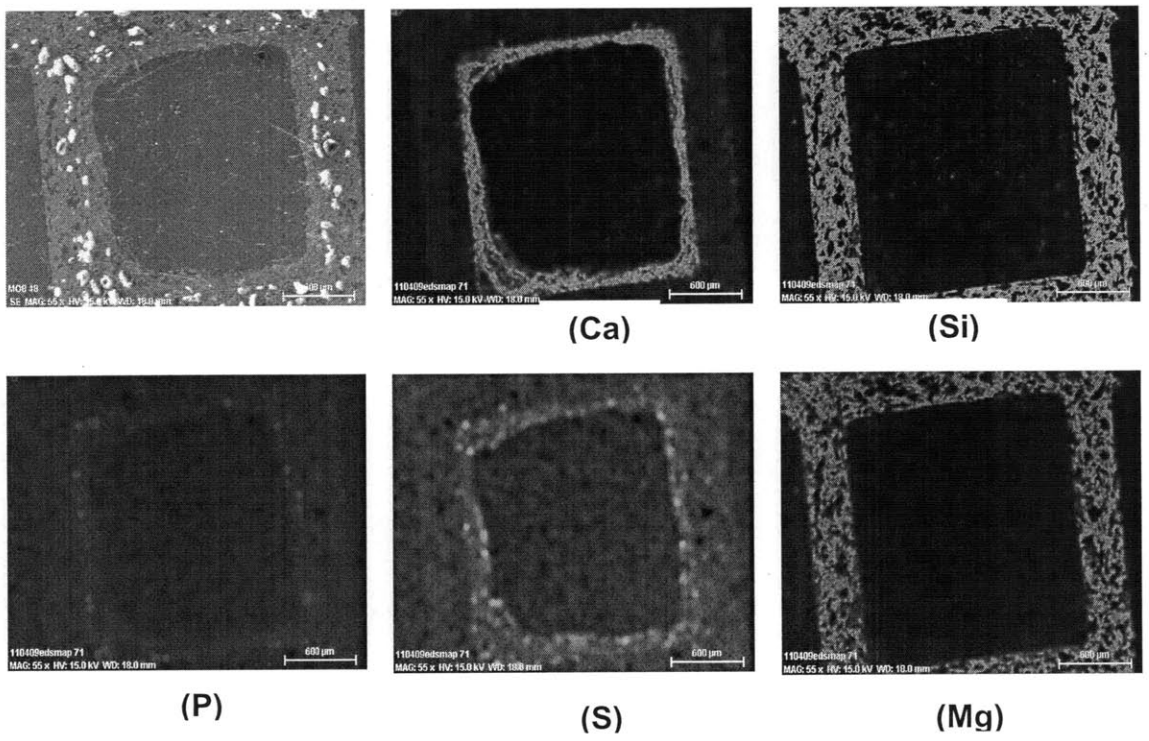

Figure 3.5. Lab- aged DPF with 29 g/L of ash from base oil and Ca additive. The white large particles on the surface of the DPF material are abrasive particles that were embedded in the epoxy during sample preparation and polishing. They do not affect the EDX analysis.

The Ca layer is the most distinct EDX image. This is expected given the high level of Ca in the oil formulation. The ash layer appears to be defined by Ca containing compounds. S is clearer than P but less well defined than Ca. The EDX image indicates elevated concentrations of S in the ash layer as opposed to the background. S coincides with the ash layer in the SEM image, suggesting the ash layer is composed of large amounts of calcium sulfate.

3.2.2 SEM and EDX Images of Surface Pore

Figure 3.6 shows a thick ash layer covers the surface pore. Most of the ash is Ca and S, which is expected for this oil formulation. The top left of the Ca image appears to have some Ca accumulation in it. The S image below it shows a high concentration region in a similar location. These images show that a small amount of calcium sulfate ash is present inside the surface pore. Relative to the amount of ash in the ash layer, this is very small.

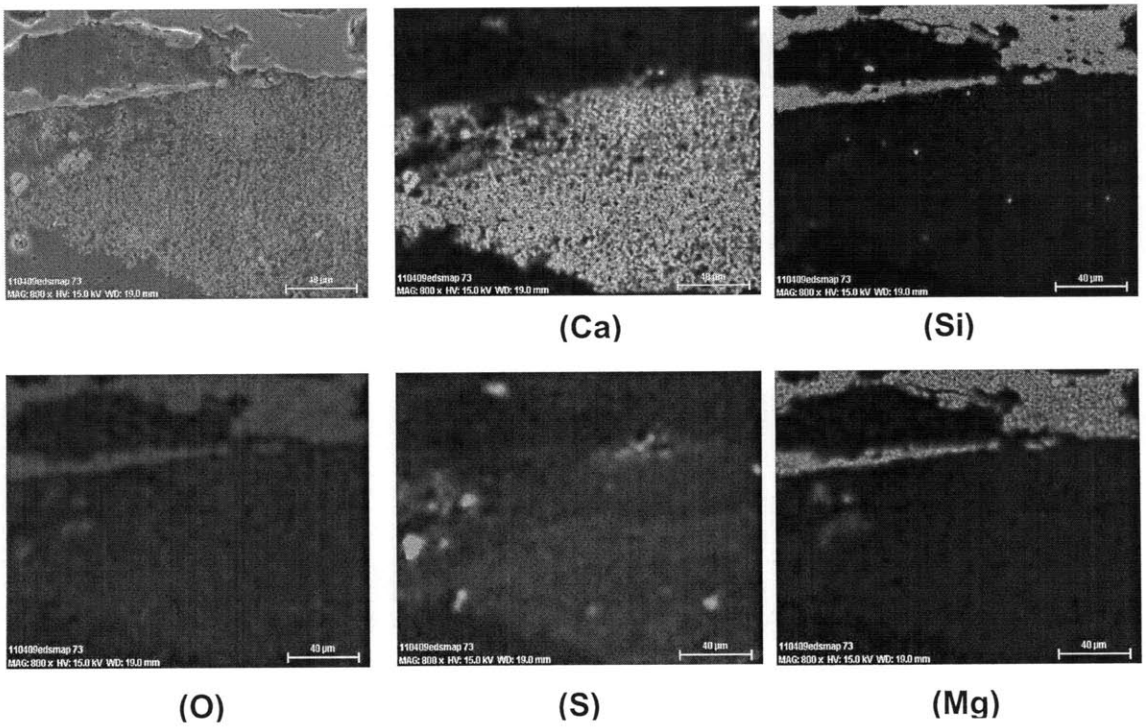

Figure 3.6. Lab- aged DPF with 29 g/L of ash from base oil and Ca additive.

3.2.3 Line Scan of Surface

Two line scans were taken of this sample for consistency. Both scan paths extend through the DPF wall material to detect ash that may have been deposited within wall pores.

The first line scan path did not reveal any ash in wall pores (Figure 3.7). There were elevated levels of Ca in the ash layer, which is expected for this oil formulation. The ash layer was approximately 200μm thick (Figure 3.8).

The second line scan path follows a different section on the DPF wall (Figure 3.9). It also leads through the entire wall and ash layer. The results are similar to those from the first path. There were very high Ca levels, and slightly elevated S levels.

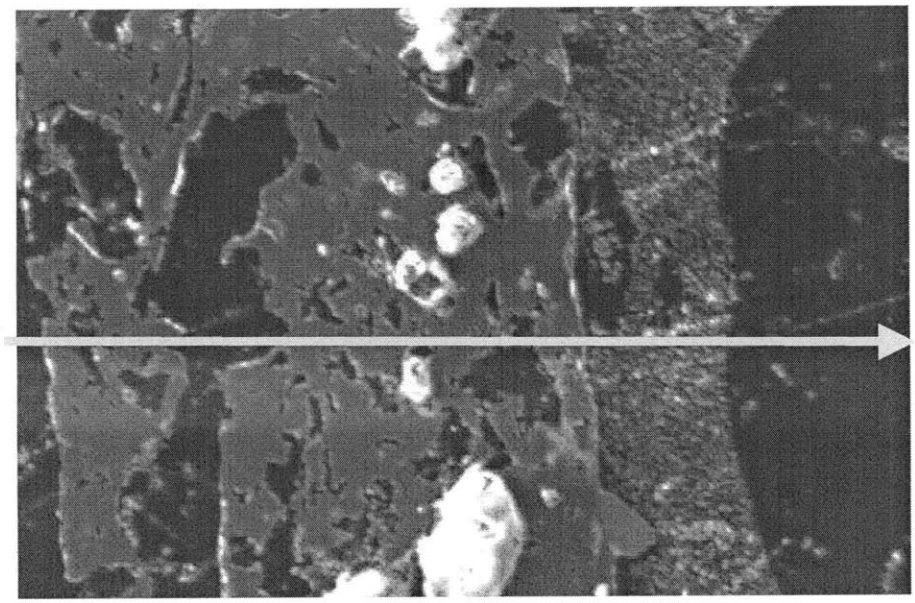

Figure 3.7. Lab- aged DPF with 29 g/L of ash from base oil and Ca additive. The line scan path for Lab- aged DPF inlet channel loaded with base oil and Ca additive. It extends from the outlet surface, through the DPF wall material, through the ash layer, and into the inlet channel.

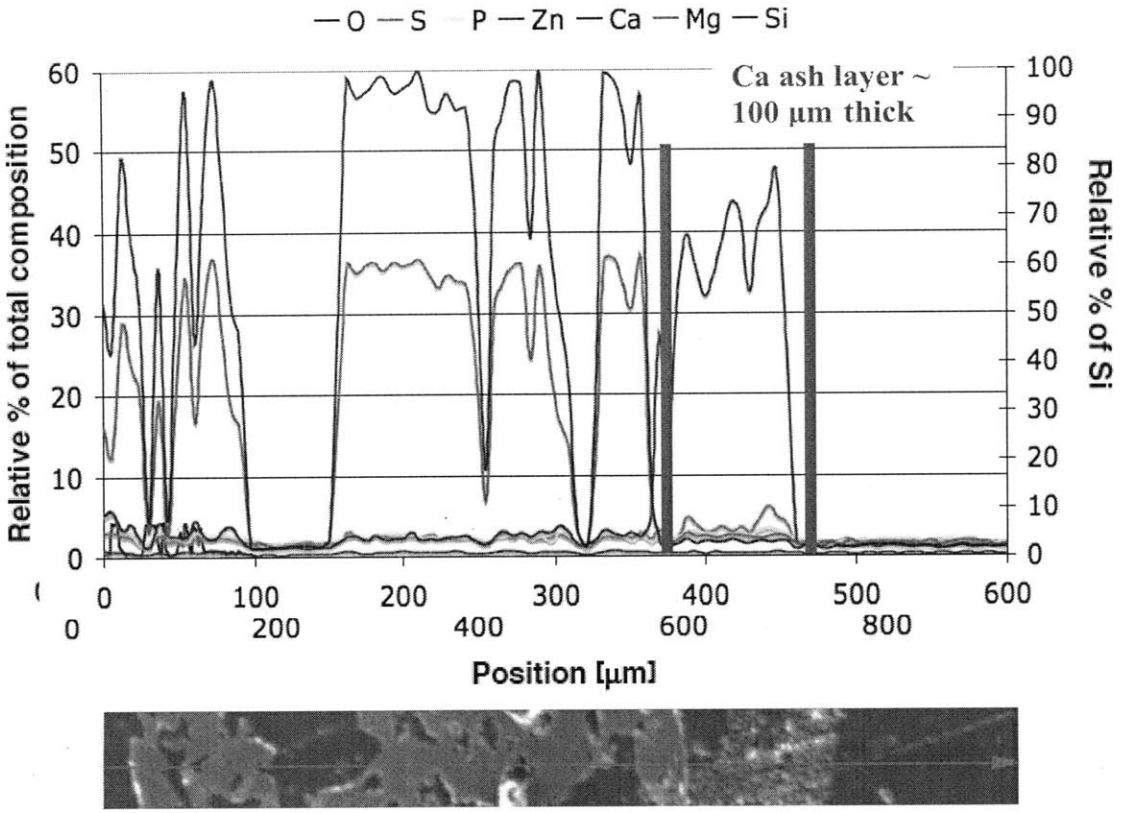

Figure 3.8. Lab- aged DPF with 29 g/L of ash from base oil and Ca additive. The scan revealed no ash accumulation in the wall. There were elevated levels of Ca in the ash layer, which is consistent with the EDX images.

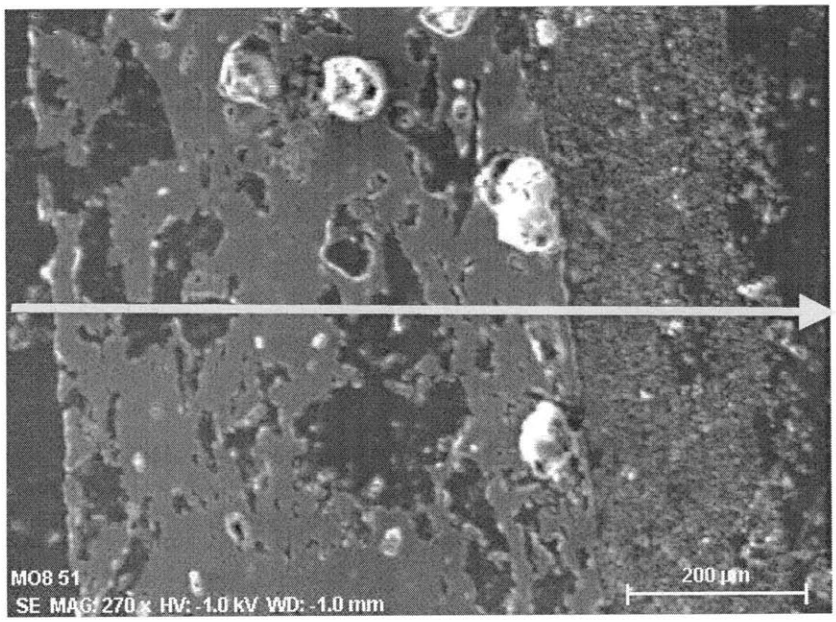

Figure 3.9. The second line scan for Lab- aged DPF with 29 g/L of ash from base oil and Ca additive.

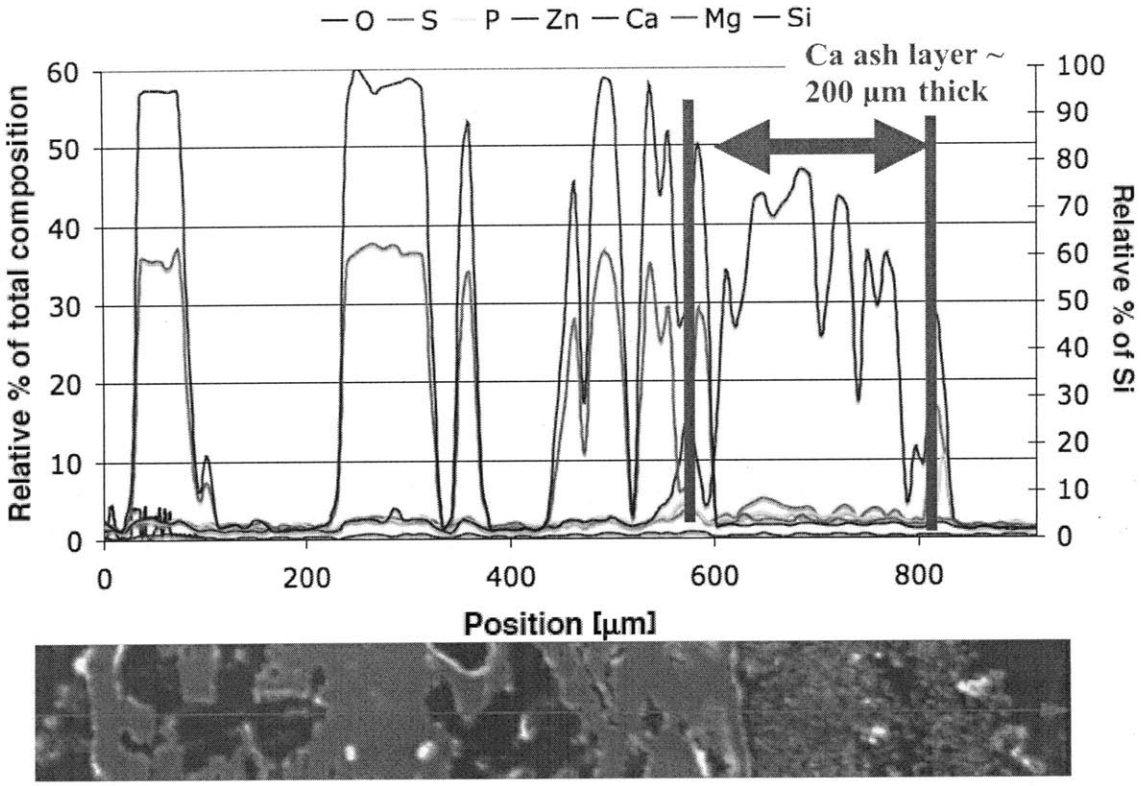

Figure 3.10. Lab- aged DPF with 29 g/L of ash from base oil and Ca additive. The second line scan reveals no ash in the wall.

3.2.4 Summary of Results for Lab- Aged DPF with Base Oil and Calcium Additive

Based on the analysis of the ash accumulation in the DPF channel, along the wall, and near surface pores, for the DPF containing only Ca- based ash, the following summarizes the general observations:

- The ash layer had a high concentration of Ca and low concentration of S.
- There was no ash accumulation found in the surface pores.
- No ash was found in the DPF wall.
- Lack of ash accumulation in surface pores and DPF wall is similar to results from. CJ-4 loaded sample, showing ash covered, but did not accumulate in surface pores.

3.3 Lab- Aged DPF with ZDDP Additive

This DPF was loaded with 28 g/L of ash from the base oil with ZDDP additive. The ash in this sample was expected to have very high levels of Zn and P because the oil formulation has over 2500ppm of both additives. The oil was formulated to 1% sulfated ash level.

3.3.1 SEM and EDX Images of Inlet Channel

There is an unexpected amount of Ca, due to some error in the preparation process. S is almost absent from the EDX, with the exception of a few S traces in high concentration regions. The Ca is better defined, with a large accumulation in the top left corner of the image (Figure 3.11). The Zn and P levels are high, which is expected. These elements appear to constitute most of the ash.

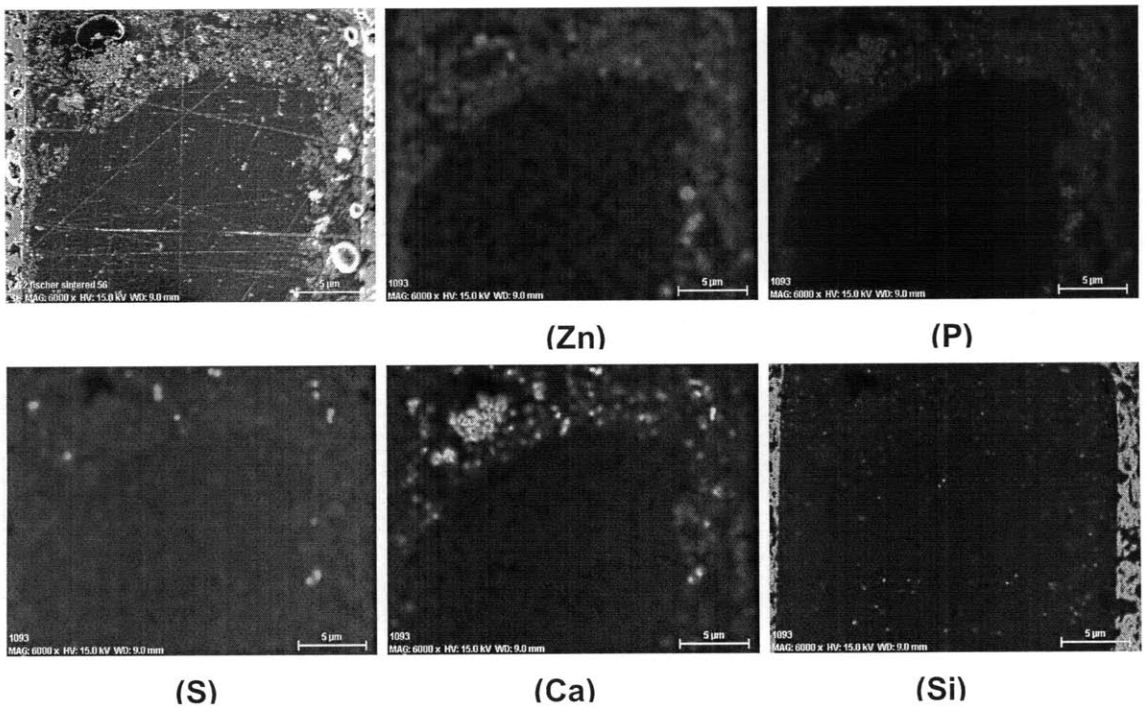

Figure 3.11. Lab- aged DPF with 28 g/L of ash from base oil and ZDDP additive.

3.3.2 SEM and EDX Images of Surface

This set of images pertained to the ash- surface pore interface. The SEM image focuses on the ash layer and the DPF channel surface. There are pockets of high concentration S and P observed. Zn and P appear to make up most of the ash (Figure 3.12).

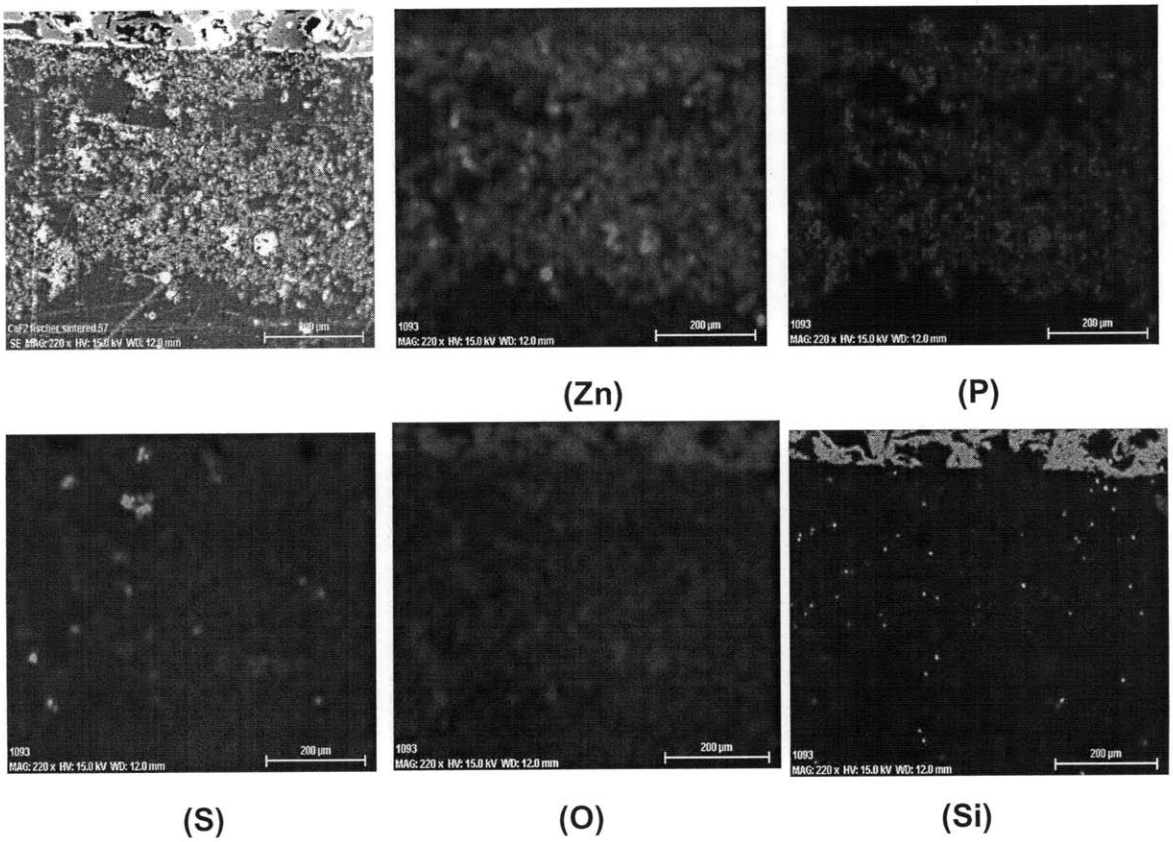

Figure 3.12. Lab- aged DPF with 28 g/L of ash from base oil and ZDDP additive.

Closer inspection of the Si and P images reveals that the P ash actually does collect in two of the largest surface pores in this sample. This is the first sample in which more than a trace amount of ash was found in a surface pore. The line on each image indicates where the DPF wall material meets the ash layer (Figure 3.13).

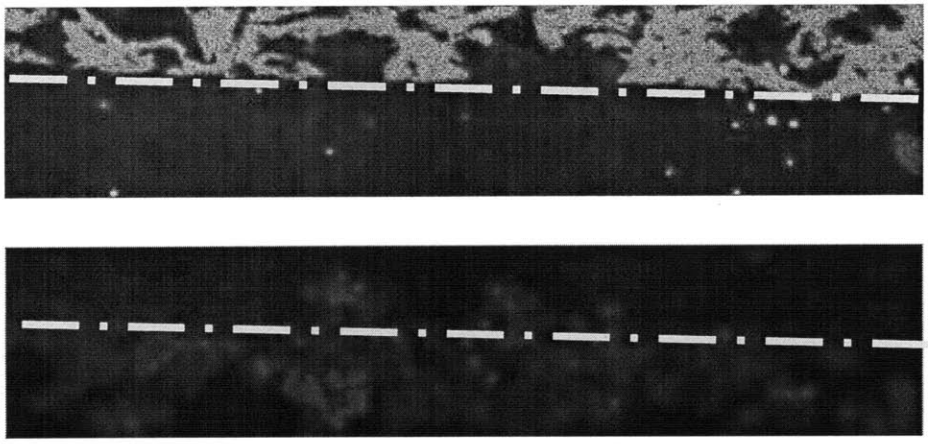

Figure 3.13. Lab- aged DPF with 28 g/L of ash from base oil and ZDDP additive. Si image (above) and the P image (below). Notice that the P EDX indicates some of the ash appears inside the two center pores.

3.3.3 SEM and EDX Image of Surface Pore

Since this is the first sample to show ash collection in the pores, it was worthwhile to look at one of the pores Figure 3.13 more closely. The EDX images show that all major additives collected in the surface pore at the center of the image. Zn is uniformly distributed in the ash layer, and in the pore. P and S have high concentration regions in the pore as well (Figure 3.14).

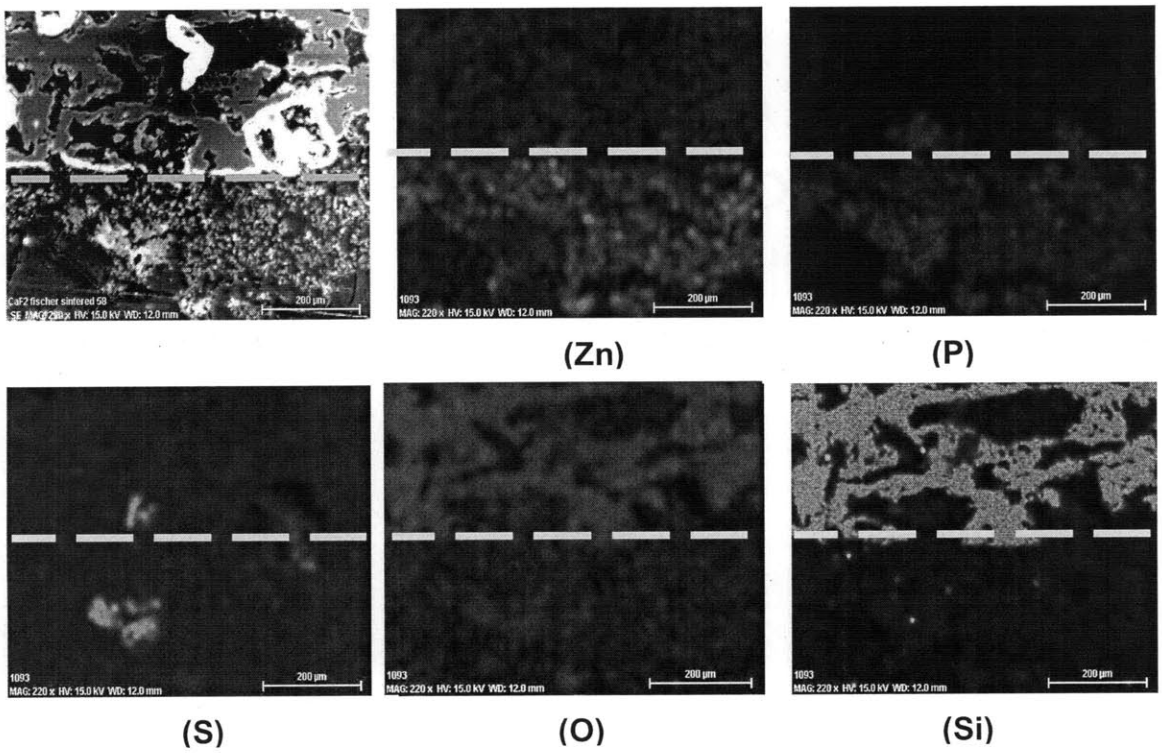

Figure 3.14. Lab- aged DPF with 28 g/L of ash from base oil and ZDDP additive, SEM image of a surface pore.

3.3.4 Line Scans of Surface Pore

The line scans were taken in the surface pore displayed Figure 3.14. The scans begin in known DPF material, go through the large surface pore, and through the ash layer (Figure 3.15). 200μm marks the halfway point inside the surface pore of interest. At this point, there was a high Zn concentration and elevated S concentration. This line scan confirms the EDX observations of ash in the pore (Figure 3.16).

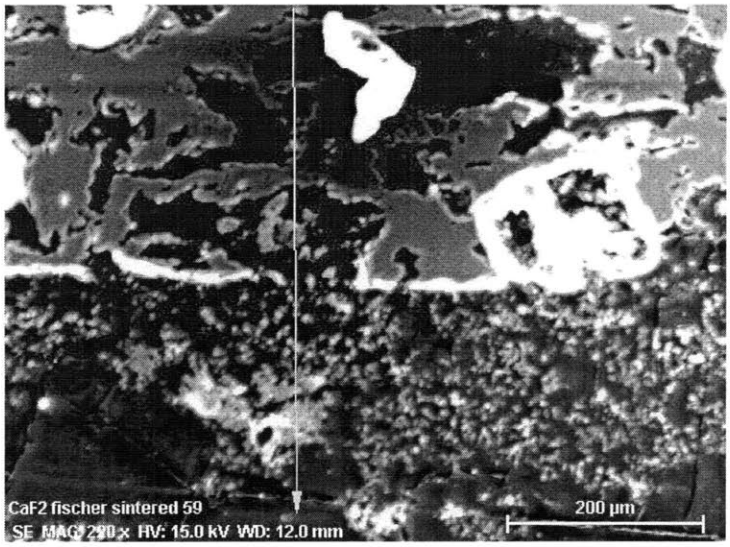

Figure 3.15. Lab- aged DPF with 28 g/L of ash from base oil and ZDDP additive. The scan path was chosen pass through the DPF surface pore.

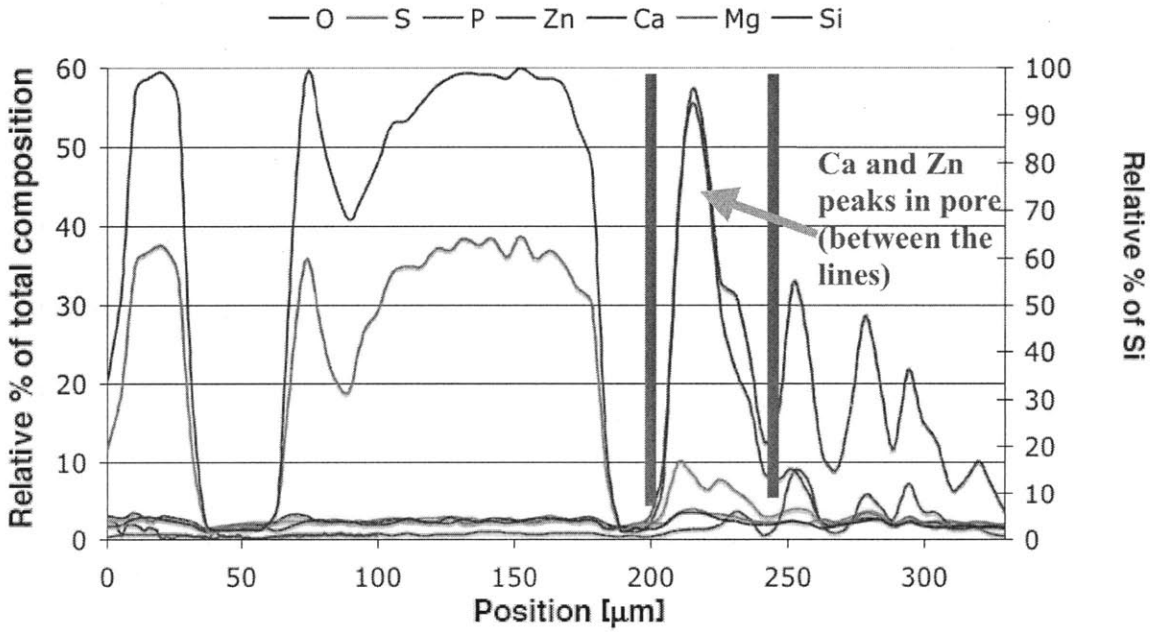

Figure 3.16. Lab- aged DPF with 28 g/L of ash from base oil and ZDDP additive. The surface pore begins at 100 µm. The ash layer begins at 250 µm. The line scan shows elevated levels of Ca and Zn and P beginning at 200 µm, which is inside the surface pore.

3.3.5 Summary of Results for Lab- Aged DPF with Base Oil and ZDDP Additive

Based on the analysis of the Zn based ash accumulation in the DPF channel, along the wall, and near surface pores, the following summarizes the general observations:

- Most of the ash is comprised of Zn and P, probably in the form of zinc phosphate
- This is the first sample in which ash is found in its surface pores. However, the sample size is too small to draw conclusions about general ash accumulation behavior in surface pores based on this observation alone. Further SEM and EDX analysis using cores from this sample DPF are warranted.

3.4 Regenerated Field- Aged DPF

This sample was taken from a DPF that had accumulated ash after approximately 180,000 miles of on road use in a heavy- duty truck using CJ-4 oil.

3.4.1 SEM and EDX Images of Inlet Channel

All major lubricant additives were found in the CJ-4 ash. This core was removed from the back of the DPF where ash completely filled the channel, forming a plug. The SEM images reveal that the channel is completely plugged with ash (Figure 3.17). The ash appears to be separated from the wall. The separation may be due to the ash shifting after the DPF was removed from the truck and shipped to MIT.

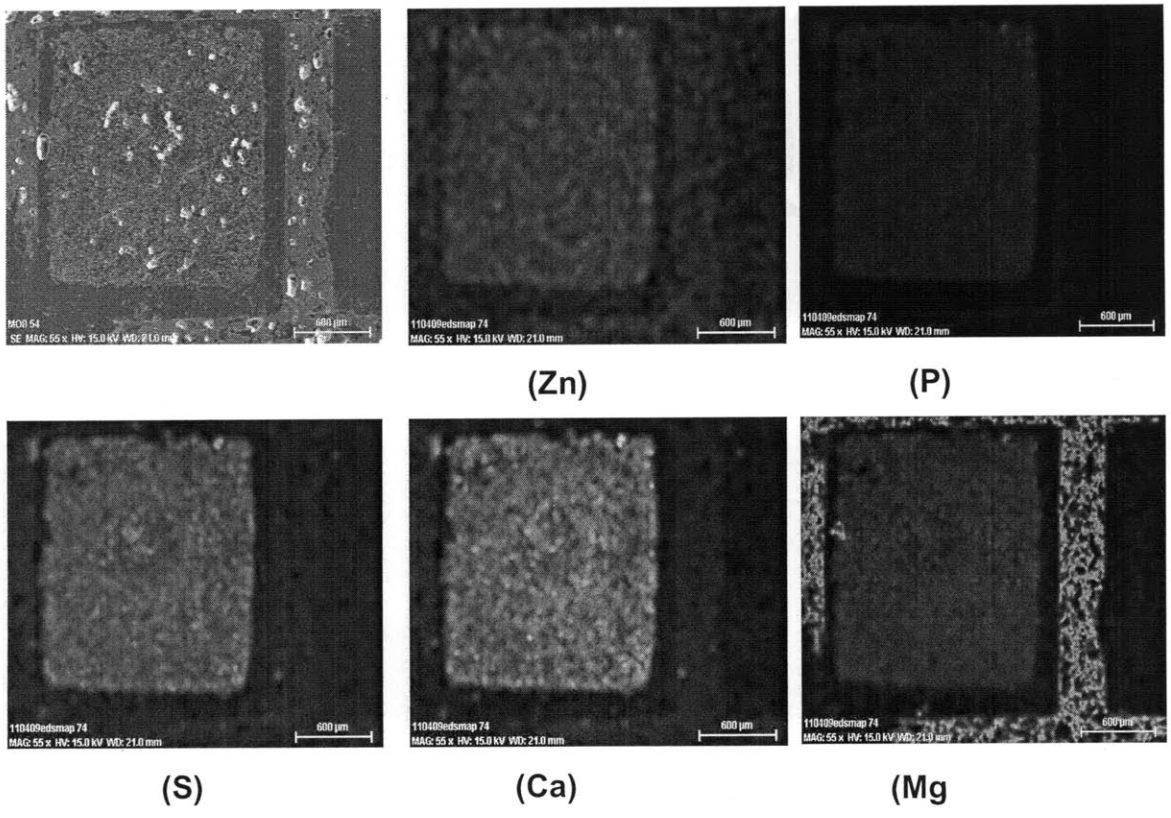

Figure 3.17. Field- aged DPF after 180,000 miles with CJ-4 oil, SEM image with EDX analysis of channel.

Ca, P, S, and Zn are significant parts of the ash. These elements are all expected in CJ-4 oil. Zn appears less concentrated than Ca, as evidenced by the intensity of the EDX image.

3.4.2 SEM and EDX Images of Channel Surface

The field samples had intact Al- based washcoats when they were prepared for imaging. The waschoat is identifiable as the relatively smooth section in the center of the image, next to the DPF surface. The Zn accumulation in the washcoat is not significant. Ca on the other hand, appears to deposit in small areas near the washcoat surface. These areas coincide with some of the high concentration regions of S deposition. S and P are unusual in that they appear to preferentially filter into the washcoat material. There is a definite increase in S concentration in the washcoat compared to its surroundings. The P accumulation is even more unusual. It appears that P prefers to accumulate on any washcoat surface that is exposed to exhaust flow (Figure 3.18).

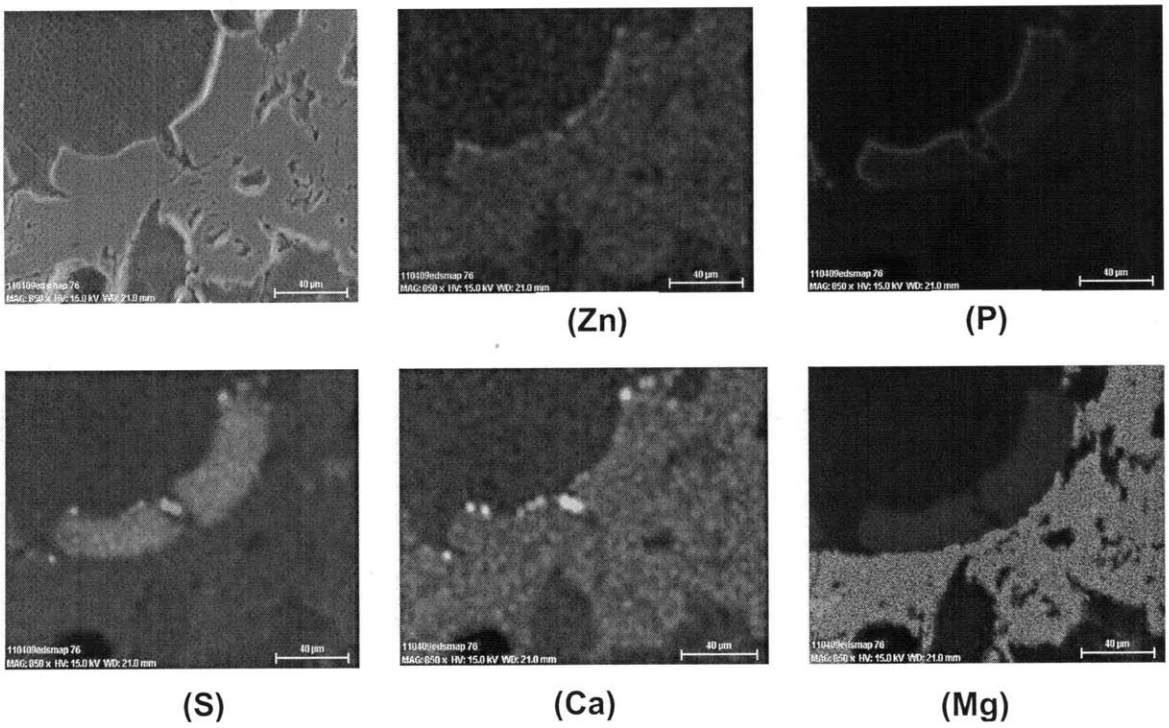

Figure 3.18. Field- aged DPF after 180,000 miles with CJ-4 oil, SEM and EDX images of Al washcoat and ash.

3.4.3 Line Scans of Washcoat

The scan path was chosen to explore the washcoat observations in the EDX images. The path begins inside a wall pore, travels through the DPF material and through the washcoat, ending in the inlet channel. There is no ash present immediately adjacent to the washcoat (Figure 3.19).

The washcoat lies between 65-90 μm on the line scan graph. The scan revealed that low levels of Ca, P, S, Zn appear in the washcoat material. There is a P peak at the 90μm, corresponding with the bright P region in the EDX images at the surface of the washcoat exposed to exhaust flow (Figure 3.20).

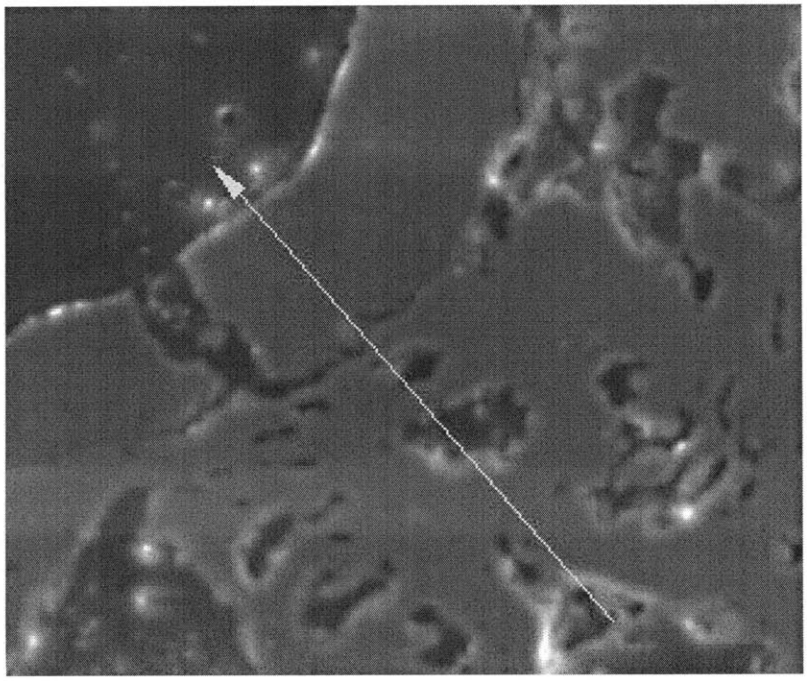

Figure 3.19. Field- aged DPF after 180,000 miles with CJ-4 oil. First line scan of washcoat travels through DPF material and washcoat, ending in the inlet channel.

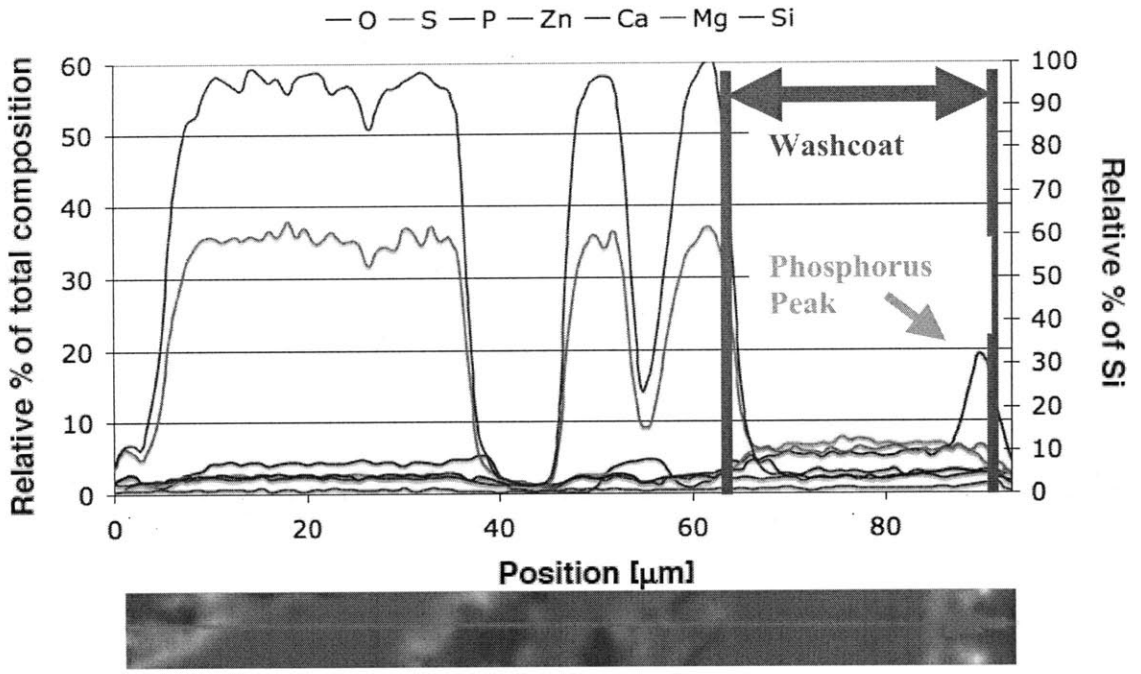

Figure 3.20. Field- aged DPF after 180,000 miles with CJ-4 oil. Ash elements were detected in the washcoat.

In the second line scan, the washcoat is defined at 27-46µm region as shown in Figure 3.21. The concentrations of Ca, Zn, P, and S are all elevated on the washcoat. The P peak observed in the previous scan is absent here, possibly due to the fact that the scan ends near the edge of the washcoat, instead of beyond it (Figure 3.22).

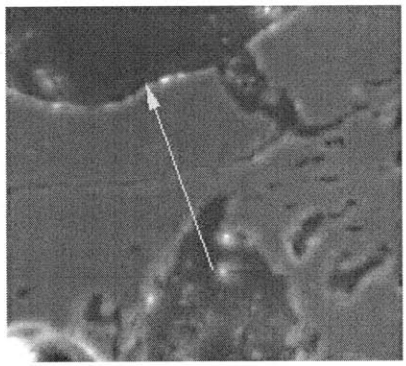

Figure 3.21. Field- aged DPF after 180,000 miles with CJ-4 oil. The second line scan path analyzes another section of the washcoat.

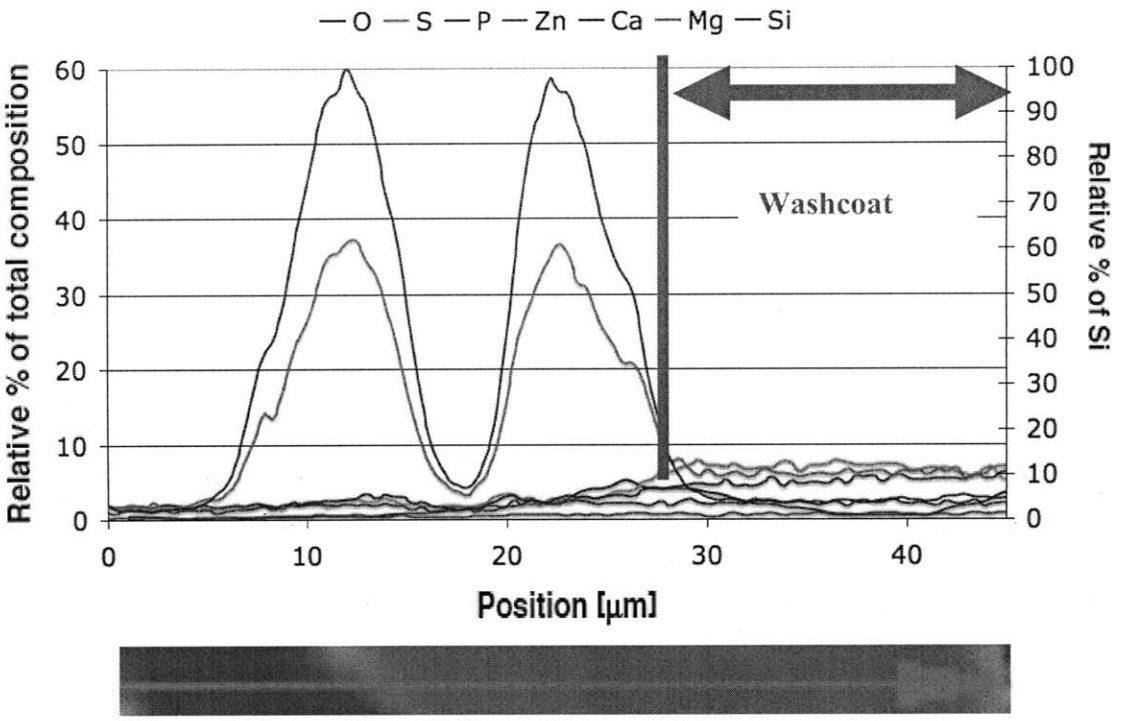

Figure 3.22. Field- aged DPF after 180,000 miles with CJ-4 oil. Elevated levels of ash elements (Ca, P, S, Zn) were detected in the washcoat. The washcoat begins at 27µm and ends at 46µm.

3.4.4 Summary of Results for Regenerated Field DPF

Based on the analysis of the ash accumulation in the field- aged DPF channel, and EDX analysis of the washcoat, the following summarizes the general observations:

- Zn was detected in the ash in similar concentration to Ca detected in the ash.
- P appeared to preferentially deposit in the washcoat. Especially high levels of P were observed on washcoat surfaces that would have been open to the flow of exhaust or in contact with the ash layer after it formed.
- All major additives were present in some amount on the washcoat surface.
- Ca and S deposits were well matched, suggesting calcium sulfate ash.
- There was no ash observed in the pores for the samples analyzed.

3.5 Un- Regenerated Field- Aged DPF

This sample came from another heavy- duty truck DPF that was removed after approximately 180,000 miles of use with CJ-4 oil. It differs from the field sample in Section 3.4 because this DPF was removed prior to its last. Unfortunately, because the samples were coated with carbon for SEM analysis, EDX cannot be used to detect PM that was left in the channel.

3.5.1 SEM and EDX Images of Inlet Channel

The expected additives for CJ-4 ash are present in the ash. S, P, and Ca accumulate uniformly in the ash layer. There is a lower, but significant amount of Zn as well. These results do not differ much from the regenerated DPF from Section 3.4 (Figure 3.23).

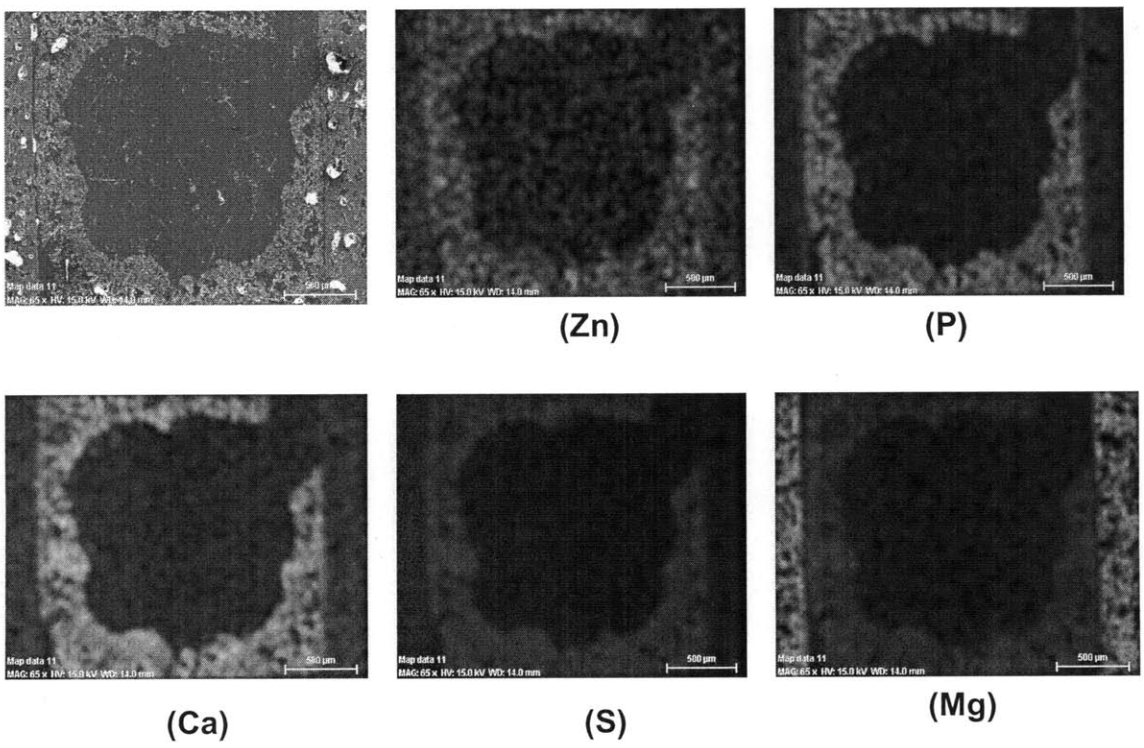

Figure 3.23. Un-regenerated field- aged DPF after 180,000 miles. Ca, Zn, P and S are all present in the ash layer as shown by the EDX images of the inlet channel.

3.5.2 SEM and EDX Images of Ash- Washcoat Interface

This sample (550x magnification) showed the ash layer remained in contact with the washcoat surface. The ash itself is composed of Zn, Ca, S, and P as expected for CJ-4 ash. This region was chosen to look at the elements that interact with the washcoat. The left of the image is the ash layer. The smooth material left of center is the washcoat. The porous material on the right is DPF wall. The S appears uniformly distributed in the washcoat layer at a lower concentration than in the ash. The P also appeared in the washcoat, with the areas of highest concentration being those in direct contact with the ash (Figure 3.24).

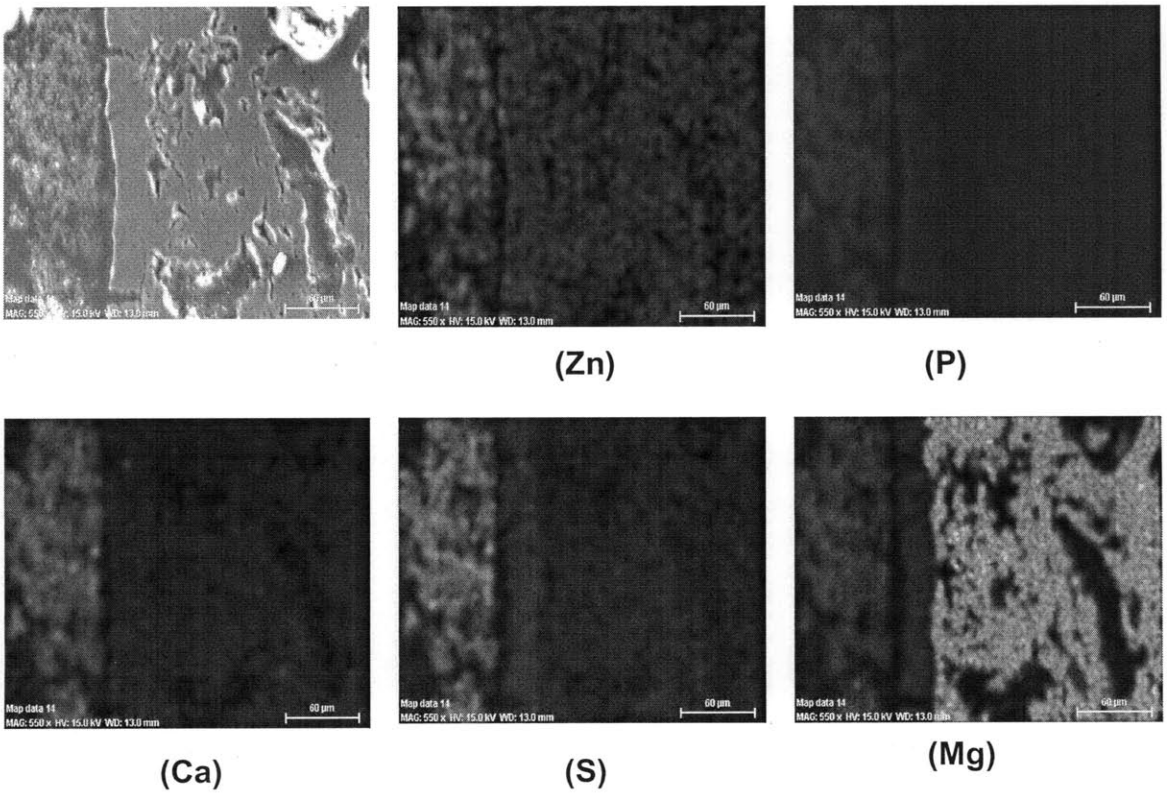

Figure 3.24. Un-regenerated field- aged DPF after 180,000 miles with CJ-4 oil. SEM and EDX images of ash, washcoat, and DPF wall interface.

3.5.3 Line Scans of Ash- Washcoat Interface

The line scan path shown in Figure 3.25 was chosen to explore the ash and washcoat chemistry. The washcoat is located between 80-100μm. There are elevated levels of P, and S in the washcoat region. There is a P peak at the edge of the washcoat- ash layer interface, which agrees with the EDX observations shown in Figure 3.26. There is also noticeable void space between 250-340μm.

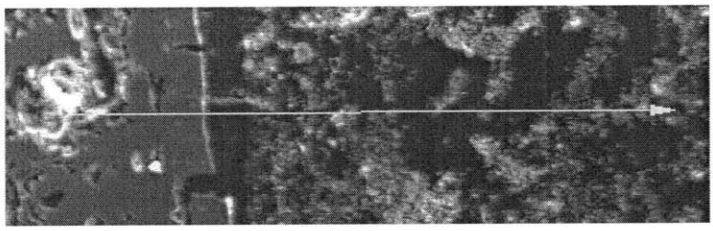

Figure 3.25. Un-regenerated field- aged DPF after 180,000 miles. The scan begins inside a DPF wall pore, goes through the washcoat, and 400 μm into the ash layer.

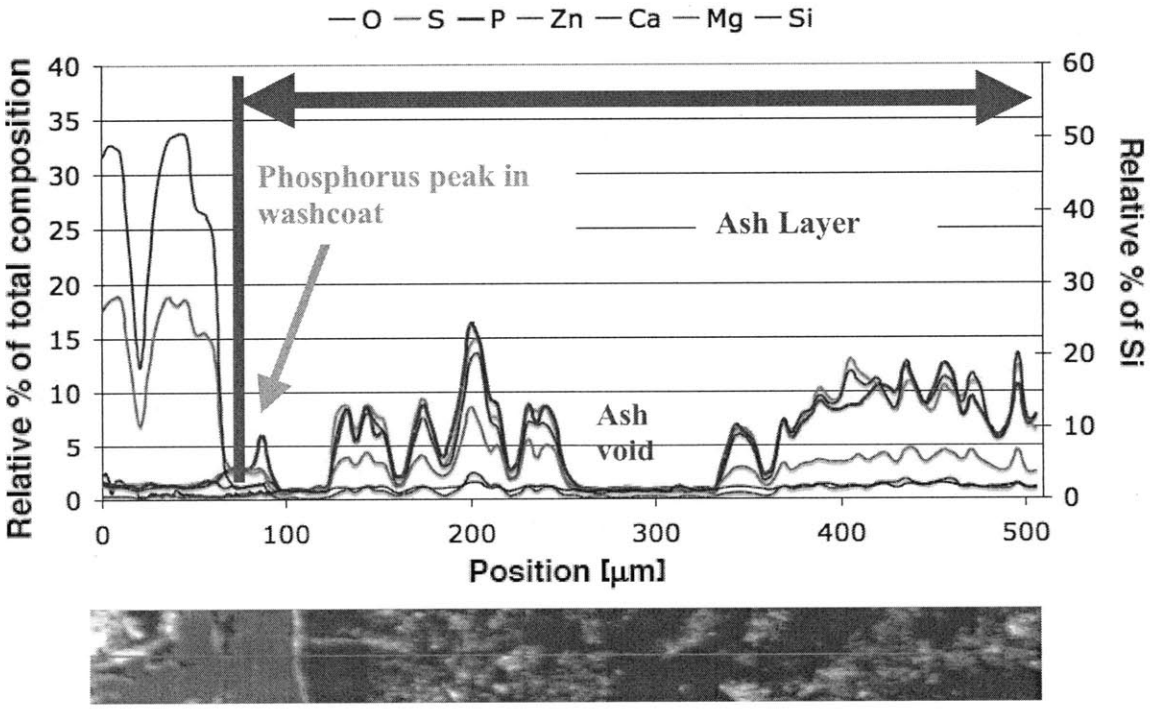

Figure 3.26. Un-regenerated field- aged DPF after 180,000 miles. The washcoat extends from between 80-100 μm.

The second line scan shown in Figure 3.27 begins inside a surface pore that is covered by the washcoat. The scan travels through the ash layer into the open channel. The

washcoat is located between 45-80 μm. There is S and P present in the washcoat, though no P peak is observed at the washcoat- ash layer interface. Unsurprisingly, since the washcoat blocks the surface pore opening, no ash is detected in it (Figure 3.28).

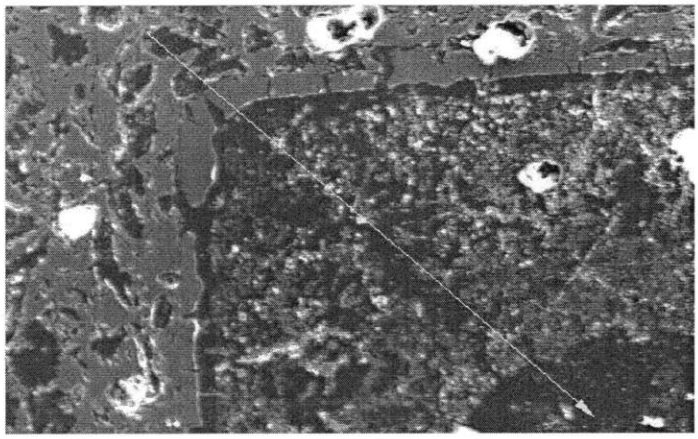

Figure 3.27. Un-regenerated field- aged DPF after 180,000 miles. Second line scan path.

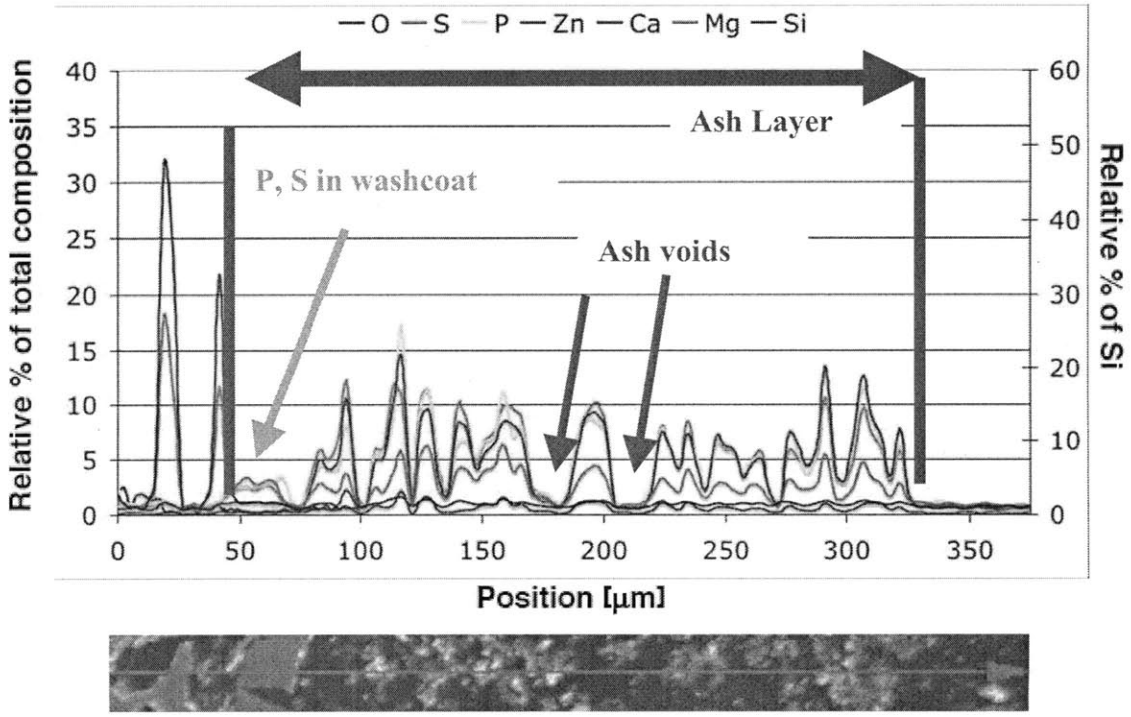

Figure 3.28. Un-regenerated field- aged DPF after 180,000 miles. P and S are present in the washcoat. The ash is composed of P, Zn, Ca, and S as expected.

3.5.4 Summary of Results for Un- regenerated Field- Aged DPF

Based on the analysis of the ash accumulation in the Field- aged DPF channel (un-regenerated), and EDX analysis of the washcoat, the following summarizes the general observations:

- Zn was detected in the ash at similar concentration to the Ca observed
- P had also accumulated. It appeared to preferentially deposit in the washcoat. High levels of P were observed on washcoat surfaces that would have been open to the flow of exhaust or in contact with the ash layer after it formed.
- All major additives were present in some amount in the washcoat.
- Ca and S deposits were well matched, suggesting calcium sulfate ash.
- There was no ash observed in the pores for the samples analyzed.
- There were void spaces in approximately 30% of the ash, based on the line scan results. The void spaces in this sample, and the others, can be used to calculate ash porosity.

4 CONCLUSIONS

Five Lab- aged and Field- aged DPF samples were examined in this study. The objective of this work was to obtain a better understanding of ash accumulation in the DPF pores, and to determine how different oil formulations affect ash accumulation. Sample cores were taken from DPFs loaded with ash either via on- road fleet testing, or using the accelerated ash loading system at MIT Sloan Automotive Laboratory. Three samples (two Field- aged DPFs and one Lab- aged DPF) were loaded with CJ-4 oil based ash. The other two lab samples were loaded with a base oil and Ca or base oil and ZDDP additive, both formulated at the 1% sulfated ash level.

The samples were imaged at the MIT CMSE using scanning electron microscopy, and analyzed with an energy dispersive X-ray. While SEM provides high- resolution images, EDX provides information related to the local elemental distribution of the sample. Although the sample size in this study was small, the analysis revealed:

- All major additives were present in CJ-4 ash loaded DPFs (Zn, P, Ca, Mg, S).
- For all of the DPFs analyzed in this study, most of the ash accumulated on the channel wall, not in surface pores.
- The line scans and SEM images show large voids in the ash layer, indicating significant porosity. The voids could be used to calculate the porosity of the ash layer.
- Line scans revealed some preferential filtering of P and S in the washcoat material in the Field- aged DPFs.

These results contribute to a better understanding of ash accumulation behavior, enabling others to improve ash accumulation models for future DPF development. Better DPFs will improve vehicle performance and fuel economy in the future.

4.1 Conceptual Description of Soot- Ash- Pore Accumulation Model

Based on the results and conclusions in this study, a theory was formulated to describe ash layer formation in the DPF inlet channel. Ash comprises of approximately 1% of total PM in diesel exhaust that initially accumulates in the DPF. SEM imaging and EDX analysis of DPF samples from Field- aged filters and Lab- aged filters revealed that very little ash accumulates in pores. Most of the ash detected creates a layer that covers the surface pores. The ash layer also covers the DPF washcoat in catalyzed samples. A conceptual description of the ash accumulation process in the DPF is shown in Figure 4.1. First, PM in exhaust fills surface pores and creates the soot cake layer (Step 1). After regeneration, ash that was in the soot cake layer is left on the DPF surface (Step 2). The ash from the previous regeneration prevents the soot cake layer from coming in contact with the DPF surface, preventing depth filtration and access to the washcoat where the ash layer has formed (Step 3). Ash from previous regenerations prevents more ash from collecting in pores. Eventually as more PM accumulates on top of the ash layer, access to the DPF material and washcoat catalyst is further restricted (Step 4). While the observations in this study support the proposed conceptual framework, additional work is warranted to more accurately quantify ash distribution and to validate this theory.

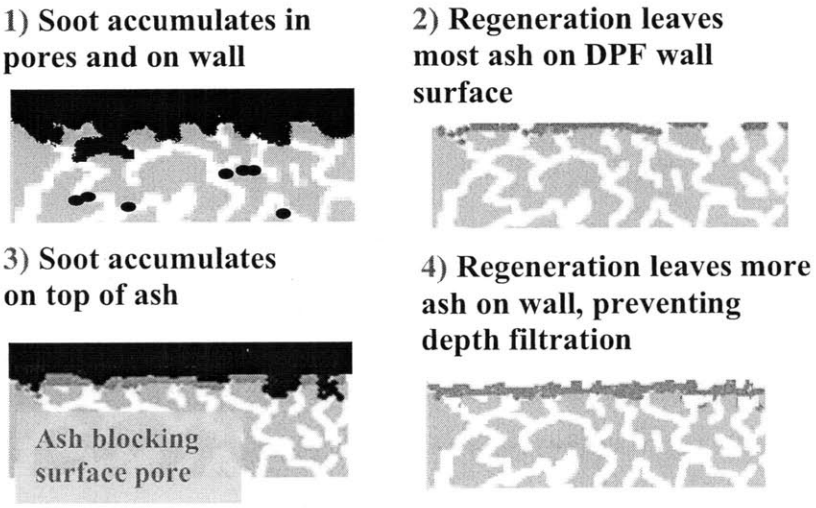

Figure. 4.1 Model of ash layer creation.

5 FUTURE WORK

While the work conducted in this study provided additional information related to ash accumulation, further research is necessary to obtain a more complete understanding of ash porosity in order to contribute more quantitative information to the DPF computer models currently being developed at MIT. Now that the mercury porosimeter is available at the MIT ISN, it is possible to take use sample cores from the DPFs tested in this study to compile porosity data. The data from the line scans indicate that there is some void space in the ash layer, which can also be used to measure porosity. Additionally, the SEM images from this work could also be used for porosity measurements via image analysis. Measuring porosity will allow future researchers to have a more complete understanding of ash related pressure drop. The results from the porosity measurements will provide quantitative data to support the qualitative observations from the image analysis presented in this study.

Additionally, the preferential accumulation of P and S in the washcoats is an interesting topic of study to determine if P and S interact similarly with other washcoat chemistries. The data complied here only identifies the phenomenon. This interaction could also affect catalyst performance. Lastly, the ZDDP Lab- aged DPF must also be revisited to determine the cause of the anomalous Ca accumulation in the ash.

On a more fundamental level, improving understanding of how each of these oil additives (Zn, Mg, Ca, P, and S) interact with the DPF substrate is essential optimizing future oil formulations. Better oil formulations produce less ash, reducing ash related pressure drop, and increasing fuel economy. DPF technology has proven to be highly effective for reducing PM emissions. Knowledge from this and other studies can be used to improve DPF service life.

6 REFERENCES

[1] Madslien, J., BBC News, "Diesel Cars Set to Outsell Petrol," <news.bbc.co.uk/2/hi/business/2332669.stm>, October 23, 2002.

[2] DieselNet Technology Guide, <http://www.dieselnet.com/tech/diesel_case.html> , 2010.

[3] Heywood, J.B., Internal Combustion Engine Fundamentals, McGraw-Hill, Inc., New York, 1988.

[4] Sappok, A., "The Nature of Lubricant- Derived Ash Related Emissions and Their Impact on Diesel Aftertreatment System Performance," Massachusetts Institute of Technology, 2009.

[5] Bowers, B., "Multi-Fuel Fuel Processor and PEM Fuel Cell System for Vehicles," SAE 2007-01-0692, 2007.

[6] United States Environmental Protection Agency, <www.epa.gov/air/airpollutants.html>

[7] Green Car Congress, "Study: Black Carbon Pollution Major Factor in Global Warming," <http://www.greencarcongress.com/2008/03/study-black-car.html>, 2008.

[8] DieselNet Technology Guide, <http://www.dieselnet.com/tech/dpf_top.html>, 2010.

[9] Jaaskelainen, H., Majewski, A.: "Diesel Engine Lubricants," <http://www.dieselnet.com/tech/lube.html#intro>, 2009.

[10] McGeehan, J., "API CJ-4: Diesel Oil Category for Both Legacy Engines and Low Emission Engines Using Diesel Particulate Filters," SAE 2006-01-3439, 2006.

[11] Karin, P., Cui, L., Rubio, P., Tsuruta, T., Hanamura, K., "Microscopic Visualization of PM Trapping and Regeneration in Micro- Structural Pores of a DPF- Wall," SAE 2009-01-1476, 2009.

[12] Deshpande, S., Kulkarni, A., Sampath, S., Herman, H., "Application of Image Analysis for Characterization of Porosity in Thermal Spray Coatings and Correlation with Small Angle Neutron Scattering," Department of Materials Science and Engineering, State University of New York at Stony Brook, 2004.

[13] Bonnie, J., Fens, T., Koninkijke/ Shell Exploratie en Produktie Laboratorium, "Porosity and Permeability from SEM Based Image Analysis of Core Material," SPE 23619, 1992.

7 APPENDIX

7.1 DPF Sample Preparation Prior to SEM

- Take DPF samples from the center of the filters since the ash accumulation is most regular in the center of the DPF (where the radius is near zero in the circular plane of the cylindrical DPF).
- The cores should be 0.5" in length.
- Coat samples in epoxy (with the face that the user wants to image placed in the bottom the dish).
    - Epoxy must be poured into the dish one drop at a time so that it does not push the ash out of the channels
- Grind the epoxy surface with 500, 1200, and 4000 grit sandpaper respectively prior to carbon coating.
- Coat with 50nm of carbon at CMSE SEM laboratory.

7.2 Important Contacts

Patrick Boisvert- CMSE- SEM and EDX Training
Rm 13-1018
Phone: 617-258-9140
Fax: 617-258-6478
Email: pboisver@mit.edu

Yinlin Xie- CMSE- Epoxy Sample Preparation
Rm 4-413
Phone: 617-253-6937
Email: xieyl@mit.edu

Kangyi Mao- ISN- Mercury Porosimeter Training
Rm: 56-454
Phone: 617-577-5550
Email: kym@mit.edu